Chapter 8

EFFECTS IN THE INNER HELIOSPHERE CAUSED BY CHANGING CONDITIONS IN THE GALACTIC ENVIRONMENT

Eberhard Möbius[1], Maciek Bzowski[2], Hans-Reinhard Müller[3], Peter Wurz[4]

1 Dept. of Physics and Space Science Center, University of New Hampshire, Durham, NH 03824, U.S.A.

2 Space Research Centre, Warsaw, Poland

3 Dept. of Physics and Astronomy, Dartmouth College, Hanover, NH, U.S.A.

4 Physikalisches Institut, Universität Bern, Bern, Switzerland

Abstract Interstellar neutral gas flows through the inner heliosphere because of the Sun's relative motion with respect to the surrounding local interstellar medium. For contemporary medium conditions, interstellar He constitutes the largest neutral gas contributor in interplanetary space at Earth's orbit. This neutral gas is the source of a small, but noticeable population of pickup ions in the solar wind, which subsequently is injected into ion acceleration processes much more efficiently than solar wind ions. In fact, He^+ has been found to be the third most abundant energetic ion species at 1 AU after H^+ and He^{2+}. During its history, the solar system must have encountered a variety of interstellar environments, including hot and dilute bubbles and much denser clouds, and will continue to do so in the future. We have studied the neutral gas and its secondary products in the inner heliosphere, such as pickup ions and energetic particles, for conditions that range from that of a hot bubble to dense clouds with densities up to 100 times the current value, allowing for variation in temperature and bulk flow velocity. We have used multi-fluid models of the global heliosphere and kinetic models of the He flow, to derive the spatial distribution of interstellar neutral H and He in the inner heliosphere. With this

P. C. Frisch (ed.), Solar Journey: The Significance of our Galactic Environment for the Heliosphere and Earth, 209–258.

limitation the termination shock is at 8 AU, an d the Earth remains in the supersonic solar wind. Except for the case when the Sun is immersed in a hot bubble with no neutral gas, interstellar He maintains its dominant role in the inner heliosphere. However, even for the highest densities, the interstellar gas generally does not yet affect the solar wind dynamically at 1 AU, except for the region of the He focusing cone on the downwind side of the interstellar flow. Because dense clouds usually are also cold, a rather narrow cone with a drastically increased density develops, which acts like a huge and stationary comet in the sense that the solar wind would be decelerated to approximately the interstellar flow speed at 1 AU. Under such conditions energetic particles generated from interstellar pickup ions would dominate the energetic particle population at least during solar minimum.

Key words: Neutral particles; pickup ions; energetic neutral atoms; energetic particles; heliosphere-ISM interaction; interstellar cloud variations

8.1 Introduction

Since the late 1960's it has been well known that the Sun's environment cannot be compared with a Strömgren Sphere, as seen around massive and luminous O or B stars. A Strömgren Sphere is basically a spherical HII region around a star in which the interstellar gas is completely ionized by the star's ultraviolet radiation, and the radius of the sphere is determined by an equilibrium between ionization and recombination at the boundary (Strömgren, 1939). Due to the Sun's motion with ≈26 km/s relative to the interstellar medium (ISM) the equilibrium condition is violated because the typical time constant for ionization of H atoms is much longer than the travel time for distances larger than a few astronomical units (e.g. Fahr, 1968a). As a consequence a wind of interstellar neutral gas blows through the entire heliosphere, which is not affected significantly by the solar wind and its embedded magnetic field. In this way, the interstellar medium fills even the inner solar system with extrasolar neutral gas. It forms a recognizable pattern with a small central void that depends on the ionization potential of the species, the interstellar flow speed and temperature, as well as the Sun's gravitation and

radiation pressure (see, e.g., reviews by Axford, 1972; Fahr, 1974; Holzer, 1977; Fahr, 2004).

Over the past 10 years, substantial attention has been devoted to potential changes in the overall size, shape and morphology of the heliosphere in response to variations in the physical parameters of the ISM environment of the Sun over time (Frisch 2000; Zank and Frisch, 1999). There has been speculation about potential effects on the Earth, in case it is exposed to the ISM rather than the solar wind (Yeghikyan and Fahr, this volume). This may happen during a very drastic compression of the heliosphere to smaller than 1 AU, which will also substantially alter the modulation of cosmic rays and thus the Earth's exposure to them (Florinski and Zank, this volume). However, less effort has been spent on

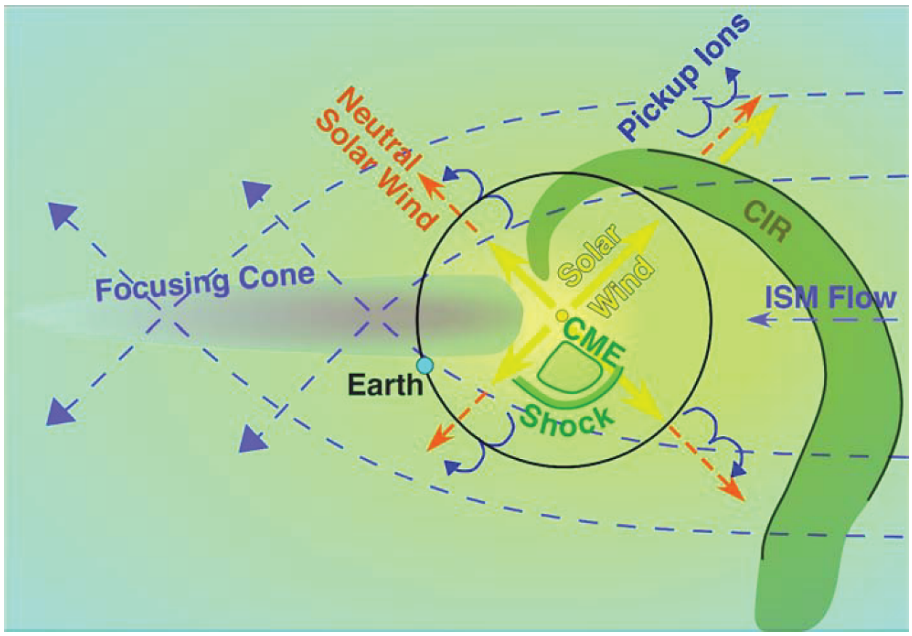

Figure 8.1. Schematic view of the inner heliosphere with the interstellar gas, its secondary particle populations, such as neutral solar wind and pickup ions, as well as their energetic offspring. The decreasing influence of the solar wind with distance from the Sun is shown in yellow and the increasing importance of the ISM in light blue.

related changes of the interstellar neutral gas inventory in the inner heliosphere in response to more moderate variations in the physical parameters of the local galactic environment. These will form the topic of the present chapter.

Throughout the heliosphere, including its innermost portion, the interstellar neutral gas flow is the source for a number of secondary products, which together with the original gas itself are important contributors to the neutral and ionized particle environment in the heliosphere. Figure 8.1 presents a view of the inner heliosphere together with the major interstellar and solar particle sources, including their secondary products and places where energetic particles are generated. Under current conditions the total density of interstellar particles dominates that of solar particles outside 5–10 AU, depending on solar activity. Through ionization by solar UV, charge exchange with solar wind ions, and electron impact ionization, interstellar pickup ions are formed that are transported radially outward with the solar wind (Vasyliunas and Siscoe, 1976; Möbius et al., 1985; Gloeckler et al., 1993). Consequently, the continuous mass-loading of the solar wind by interstellar ions leads to a slow-down beyond 30 AU (Richardson et al., 1995; Lee, 1997; Wang and Richardson, 2003). Already here the pressure of pickup ions starts to dominate in the interplanetary plasma and shows up as the leading cause of internal variations in the solar wind (Burlaga et al., 1996). In addition, pickup ions have been identified as a potent source population for accelerated particles in interplanetary space. In fact, they are accelerated in interplanetary space more efficiently by a factor of 100–200 over solar wind distributions at coronal mass ejection (CME) driven shocks and in co-rotating interaction regions (CIR), shown in Fig. 8.1 (Gloeckler et al., 1994; Chotoo et al., 2000; Möbius et al., 2001). He^{+} that originates from interstellar pickup ions is, with $He^{+}/He^{2+} \approx 0.06$, the third most abundant energetic ion species in the inner solar system (Kucharek et al., 2003). Last but not least, charge exchange between the solar wind and interstellar gas in the heliosphere not only produces pickup ions, but also leads to the generation of a small yet recognizable fraction of neutral solar wind (e.g. Fahr, 1968b; Gruntman, 1994; Gruntman, 1997; Collier

et al., 2001). Increase of the neutral gas population in the inner heliosphere due to changes in density, velocity, and temperature of the surrounding medium will, therefore, lead to an increase in the importance of each of the aforementioned secondary products. The influence of interstellar pickup ions on the solar wind dynamics will be pushed closer to the Sun. The increased density of pickup ions is mirrored in an increased importance of the relevant energetic ion populations. Finally, neutral solar wind is not blocked by the Earth's magnetic field and, thus, will have direct access to interaction with the upper layers of the Earth's atmosphere. If the neutral solar wind flux reaches a certain level, substantial effects on the particle and energy balance in the upper atmosphere are expected (Bzowski et al., 1996; Yeghikyan and Fahr, 2004). In extreme cases the interaction with the neutral solar wind may look more like the direct exposure of the Venusian or Martian atmosphere to the solar wind (Breus et al., 1989), except for the magnetic pile-up.

The purpose of this chapter is not to go into detail about the effects of all these secondary products on the Earth and the Earth's magnetosphere, which are covered in the chapters by Yeghikyan and Fahr (this volume) and by Parker (this volume). It will rather describe how the primary neutral gas distributions and the related secondary products change in response to variations in the local interstellar medium over a significant and reasonable range in interstellar density, temperature, and velocity. For the purpose of this book we will include the bandwidth of current solar activity in the range of parameters, but potential changes in the activity level with the age of the Sun go beyond the scope of this chapter. We will start the discussion with a summary of the current understanding of the interstellar inventory in the heliosphere, including knowledge about its secondary products, based on observations and heliospheric modeling. In the following section we will model changes in the hydrogen (H) and helium (He) inventory for similar sets of parameters. These two key species are kept separate because of their genuinely different interaction with the heliosphere. Helium passes through the heliospheric boundary unimpeded and is the dominant interstellar species at 1 AU because of its high ionization potential. Hydrogen is substantially filtered in the heliospheric interface region, leading to a reduction in density, slowdown, and heating. As the majority component in the ISM, H plays

the dominant role in the determination of the overall size and shape of the heliosphere. Finally, after establishing the ISM neutral distribution under these circumstances, we will discuss the effects of their variation on all the secondary products.

8.2. Observations and Modeling of Neutrals in the Contemporary Heliosphere

As has been pointed out in the introduction, neutral interstellar gas flows through most of the heliosphere. This gas flow is responsible for a number of secondary products, which can affect the environment of the Earth if their fluxes reach a high enough level. On the other hand, the presence of the neutral gas flow enables the use of powerful in situ diagnostic tools to study the gas and its products in the inner solar system, from Earth orbiting and interplanetary spacecraft. In the following we will summarize our knowledge of the interstellar neutral gas and its products under current interstellar boundary conditions.

8.2.1 Modeling of Interstellar Neutral H and He Gas in the Heliosphere

The most abundant element both in the solar wind and in the local interstellar medium is hydrogen, which consequently also determines the overall dynamics between both domains. The interaction of the solar wind plasma with the ionized component of the interstellar wind creates the heliosphere with its characteristic heliospheric boundaries, namely, the termination shock and the heliopause. The ISM plasma experiences the heliosphere as an obstacle and flows around it, the heliopause being the separation surface between the solar wind and interstellar plasma. Before the supersonic solar wind reaches the heliopause, it is decelerated and heated at the termination shock and then turned into a tailward flow relative to the interstellar neutral gas (ISN) flow. Other species of the neutral gas mostly follow the bulk flow, but are dynamically decoupled because the mean free path length for collisions exceeds or is of the order of the size of the heliosphere.

Close to the Sun the ISN that flows into the heliosphere is depleted due to photo-ionization by solar UV radiation, charge exchange with solar wind ions, and electron impact ionization. The newborn ions are picked up by the interplanetary magnetic field (hence pickup ions) and are swept away with the solar wind. They will be discussed in detail further down in this section. The local loss rate of neutral particles at 1 AU is

$$\begin{aligned} -\frac{dn_{ISN}}{dt} &= n_{ISN} n_{SW} v_{rel} \sigma_p(v_{rel}) + n_{ISN} n_{SW} v_{rel} \sigma_e(v_{rel}) + n_{ISN} \beta_{phot} \\ &= n_{ISN} \left(\beta_p + \beta_e + \beta_{phot} \right) = n_{ISN} \beta_A \end{aligned} \tag{8.1}$$

where n_{ISN} is the ISN density, n_{SW} is the solar wind plasma density ($n_p \approx n_e \approx n_{SW}$), and v_{rel} is the relative speed between the interacting particles. The individual losses of neutral particles (β_p, β_e, and β_{phot}) are combined into a total loss rate β_A for each species A. The resulting change in density of the interstellar neutrals at distance r from the Sun is then given as

$$\frac{d\, n_{ISN}}{dl} = -n_{ISN} \beta_A \frac{1}{v_{ISN}} \left(\frac{r_E}{r} \right)^2 \tag{8.2}$$

where v_{ISN} is the velocity of the interstellar gas in the heliosphere and β_A is the total ionization rate for species A at Earth's orbit, i.e., at distance r_E. An inverse quadratic dependence with distance from the Sun is implemented in Eq. 8.2, which is adequate for photo-ionization and charge exchange, while electron impact usually is only a small contribution. For a first estimate the remaining fraction of neutral interstellar gas at distance r from the Sun results from integrating the ionization along the particle trajectory, based on a cold model of the ISN gas (Vasyliunas and Siscoe, 1976).

$$n_{A,ISN}(r,\theta) = n_{A,\infty} \exp\left(-\frac{\beta_A r_E^2}{v_{ISN} r} \frac{\theta}{\sin\theta} \right) \tag{8.3}$$

θ is the angle of position relative to the upwind direction and $n_{A,\infty}$ is the interstellar gas density of species A outside the influence of the Sun (i.e., the neutral density at "infinity"). It should be noted that the use of a cold model is justified in the upwind direction, while the ISN distribution on the downwind side is substantially influenced by the gas temperature. We present simple analytical relations based on the cold model here so that the reader may use them for order of magnitude estimates of the global effects of interstellar environment variations. Equation 8.3 contains the assumption that v_{ISN} does not vary with distance and the interstellar gas density does not change other than through ionization. A constant v_{ISN} approximately applies to the hydrogen flow, for which $\mu \approx 1$ (Bzowski, 2001) (μ being the ratio between radiation pressure and gravitation). Using the cold model approach of Eq. 8.3 and a total ionization rate for H in the range $_H = (3.5 \quad 8.0) \bullet 10^{\ 7} s^{\ 1}$ (a typical variation with solar activity) leads to a remaining fraction of ISN hydrogen in the upwind direction ($\theta = 0$) at Earth's orbit ranging from 0.092 to 0.0042 and from 0.62 to 0.34 at Jupiter's orbit under current interstellar medium conditions. Towards the downwind direction the remaining neutral fractions become very small inside a few AU, and the depleted volume of interstellar gas is often referred to as the ionization cavity of the Sun, although the evacuation of interstellar atoms from the ionization cavity is not complete.

The effective inflow velocity of H is lowered to ≈ 22 km/s from the original ISM value of 26 km/s because of the strong interaction of H at the heliospheric interface, as observed through the Doppler shift of the backscattered Ly α radiation (Clarke et al., 1998; Quémerais et al., 1999). In the decelerated plasma just upwind of the heliopause, charge exchange creates a density enhancement of slow neutral H, the so-called hydrogen wall, also seen in absorption in high-resolution spectra of neighboring stars (e.g., Wood et al. 2000). Neutral H atoms that enter the hot heliosheath (the region between the heliopause and the termination shock) experience charge exchange losses (Ripken and Fahr, 1983; Fahr, 1991; Osterbart and Fahr, 1992; Baranov and Malama, 1993; Izmodenov et al., 1999; Müller et al., 2000; Izmodenov et al., 2004). Charge exchange in this region provides both a cooling mechanism in the heliosheath, and heating for the region upwind of the heliopause through

secondary charge exchange of the neutrals created in the heliosheath. This also produces a hot neutral H distribution with a low bulk velocity, which leaks into the heliosphere and mixes with the remainder of the original ISN H flow to form a combined decelerated and heated neutral gas distribution. Overall the neutral H density inside the heliopause is substantially depleted from its value in the pristine ISM, known as filtration of the incoming neutral gas. Therefore, inferring the ISM H (and O) parameters from heliospheric observations is strongly model dependent.

Heavier atoms experience gravitational acceleration when approaching the Sun, as radiation pressure is negligible for them and thus $\mu \approx 0$ applies. Making use of energy conservation along the trajectory, a relation that is modified from Eq. 8.3 is derived.

$$n_{A,ISN}(r) = n_{A,\infty} \exp\left(-\frac{\beta_A r_E^{\,2}}{v_{ISN}} \delta\left(\sqrt{1+\tfrac{2}{\delta r}} - 1\right)\right) \text{where}: \delta = \tfrac{v_{ISN}^2}{M_S G} \qquad (8.4)$$

Here M_S is the mass of the Sun and G the gravitational constant. The validity of Eq. 8.4 is restricted solely to the upwind axis. Using as a reasonable range over solar activity for the He ionization rate of $_{He} = (6 \quad 20) \cdot 10^{-8} s^{-1}$ (McMullin et al., 2004), the fractional He density at 1 AU in the ISN upwind direction is $0.79 - 0.45$ at Earth's orbit and $0.95 - 0.90$ at Jupiter's orbit. The values for $_{He}$ are variable also on shorter time scales; they change with solar UV flux as well as with solar wind parameters (e.g. Rucinski et al., 1996; Bzowski 2001; Lallement et al., 2004b; McMullin et al., 2004; Witte et al., 2004), but it is sufficient to use averaged values here.

All species except H form a region of increased interstellar gas density, the focusing cone, downwind of the Sun, which is a result of gravitational bending of the particle trajectories, as indicated in Fig. 8.1. H does not show such focusing because its gravitational attraction is essentially compensated by radiation pressure and $\mu \approx 1$, or even $\mu > 1$ for high solar activity. This focusing cone has been extensively studied for interstellar He because significant density enhancements are observed already at Earth's orbit (Gloeckler et al., 2004; Möbius et al., 1995, 2004). Heavier atoms are also gravitationally focused by the Sun, but at larger distances (Gloeckler and Geiss, 2001).

A more detailed model that takes into account the random motion in a hot gas is used, from this point on, for the evaluation of the neutral He gas variations in the inner heliosphere. In particular the focusing cone cannot be adequately described with a simple cold gas approximation. In such models the density of the interstellar helium gas at a given point in space, described by the heliocentric distance r and the angular distance from the upwind axis θ, is calculated as an integral of the local distribution function $f_{ISN}(r,\theta,\mathbf{v})$ of the ISN gas. In a first step, an intermediate distribution function $f_{ISN0}(\mathbf{v}(r,\theta))$ is computed by applying Liouville's theorem along Keplerian trajectories to the distribution function $f_{\infty}(\mathbf{v}_0)$ of the unperturbed gas outside the heliosphere (assumed as a Maxwellian shifted by the bulk flow vector $\mathbf{v}_{ISN}$ of the ISN).

$$f_{\infty}(\mathbf{v}_0) = \left(\frac{m}{2\pi\, k\, T}\right)^{3/2} \exp\left[-\frac{m\left(\mathbf{v}_0 - \mathbf{v}_{ISN}\right)^2}{2kT}\right] \tag{8.5}$$

To account for ionization losses on the way, $f_{ISN0}(\mathbf{v}(r,\theta))$ is multiplied by the survival probability $E(r,\theta,\mathbf{v})$ according to

$$f_{ISN}(r,\theta,\mathbf{v}) = f_{ISN0}(\mathbf{v}(r,\theta))\, E(r,\theta,\mathbf{v})\,. \tag{8.6}$$

The survival probability is computed as

$$E(r,\theta,\mathbf{v}) = \exp\left[-\int_{t}^{\infty} \beta_{He}(r_E)\left(\frac{r_E}{r'(r,\theta,\mathbf{v},t')}\right)^2 dt'\right]. \tag{8.7}$$

$r'(r,\theta,\mathbf{v},t)$ is the heliocentric distance of an individual atom following a Keplerian trajectory from outside the heliosphere to a location (r, θ). $\beta_{He}(r_E)$ is the total ionization rate of the He atoms at 1 AU. The velocity vector of an individual atom $\mathbf{v}_0(r,\theta)$ is calculated by tracing the trajectories backwards from the point of observation.

The modeling shown here was performed assuming a time-invariable ionization rate that depends on the heliocentric distance as $1/r^2$ and is

equal to 10^{-7} s^{-1} at 1 AU, a value representative of the average present-day photo-ionization rate (McMullin et al., 2004). Apart from the EUV ionization rate, close to the Sun (inside ≈2 AU) another ionization mechanism, electron impact (Rucinski and Fahr, 1989, 1991), needs to be taken into account. The dependence of its rate on the heliocentric distance has usually been described by $1/r^{\alpha}$, where $\alpha \neq 2$ (Rucinski and Fahr, 1991). Departure from the $1/r^2$ law is mainly due to the variation of the electron temperature with heliocentric distance (Pilipp et al., 1987a,b; Marsch et al., 1989), which scales as $T_e \propto r^{-\gamma}$, with the limiting values $\gamma = 0$ and 4/3. The exact value of γ seems to vary with heliocentric distance and also with the regime (fast or slow) of the solar wind (McMullin et al., 2004) and consequently with the phase of the solar cycle. However, contributions from electron ionization remain less than that of photo-ionization, even inside 1 AU.

The EUV ionization rate varies over the solar cycle by a factor of ≈3 (McMullin et al., 2004), which leads to He density variations whose amplitude decreases with heliocentric distance and depends on the offset angle from the upwind direction (Rucinski et al., 2003). Outside the cone, this amplitude is ≈ 25% at 1 AU and ≈ 10% at 5 AU. On the cone axis the variations are much stronger, with amplitudes of ≈80% at 1 AU and ≈ 25% at 5 AU.

8.2.2 Observation of Interstellar Neutral H and He Gas in the Heliosphere

Interstellar He was first observed in the inner heliosphere through resonant backscattering of the solar He I 58.4 nm line with rocket-borne (Paresce et al., 1974) and satellite-borne (Weller and Meier, 1974) instrumentation. Density, bulk flow speed, and temperature could be deduced from the total intensity of the glow, as well as the relative intensity and width of the focusing cone, after this structure was modeled with a hot gas distribution (e.g. Fahr et al., 1978; Wu and Judge, 1979). Over many years the derived parameters varied substantially from observation to observation and carried large uncertainties (see compilations by Chassefière et al., 1986; Möbius et al., 1993). The results from the He UV observations were significantly improved when EUVE, with its low

Earth orbit, provided the opportunity to measure the He velocity distribution by using the Earth's exosphere as a natural gas absorption cell (Flynn et al., 1998). In addition, the discovery of interstellar He pickup ions at 1 AU (Möbius et al., 1985) introduced a first in situ method to probe interstellar particles and to deduce the interstellar He flow parameters (Möbius et al., 1995). Meanwhile, helium is probably the best-measured species of the inflowing interstellar gas since it is detected directly with suitable instrumentation, i.e., the GAS instrument on the Ulysses mission (Rosenbauer et al., 1983). The most recent and most advanced analysis of the GAS data gives for the bulk speed $v_{He\infty} = 26.3 \pm 0.4$ km/s (He is accelerated when approaching the Sun, $v_{He,\infty} = v_{ISN}(r = \infty)$), the flow direction in ecliptic longitude $\lambda_\infty = 74.7^\circ \pm 0.5^\circ$ and ecliptic latitude $\beta_\infty = -5.2^\circ \pm 0.2^\circ$, and the temperature $T_{He\infty} = 6300 \pm 340$ K (Witte, 2004). Since He does not interact at the boundary of the heliosphere, this set of physical parameters is considered valid for all interstellar gas species outside the influence of the Sun. The interstellar He density of $n_{He\infty} = 0.015$ cm^{-3} has been derived from Ulysses/GAS neutral He data (Witte, 2004) and from Ulysses/SWICS He^{2+} pickup ion observations (Gloeckler et al., 2004), with a smaller (10%) uncertainty based on pickup ions, because this method does not require an absolute instrument calibration. Similar flow vector and temperature values are derived for He from observations of backscattered solar He I 58.4 nm line emission (e.g. Lallement et al., 2004b; Vallerga et al., 2004). For He these different methods are compared by Möbius et al. (2004) and show good agreement in the derived parameters.

For interstellar hydrogen so far no direct neutral gas observations are available. The Ulysses/GAS instrument is not sensitive to H. Suitable instruments for the direct detection of interstellar H have only been developed recently (Wieser et al., 2005), and are currently being implemented for a space mission (McComas et al., 2004). However, starting with the analysis of backscattered solar Lyman α intensity sky maps (Bertaux and Blamont, 1971; Thomas and Krassa, 1971), the parameters of ISN H became accessible. Based on early modeling using a cold interstellar gas flow (e.g. Blum and Fahr, 1970; Holzer and Axford, 1971; Axford, 1972; Fahr, 1974), the general flow direction and an order of magnitude estimate for the density could be deduced. Through the Doppler effect, high-resolution profiles of backscattered Ly α from Copernicus provided a first reasonable value for the H bulk speed inside the

heliosphere (≈22 km/s) and constraints on the temperature (Adams and Frisch, 1977). Substantial progress towards the kinetic parameters was made with the use of hydrogen absorption cells, which provide the best information on the H flow velocity vector ($v_{H\infty}$ = 18–22 km/s, λ_∞ = 74º and β_∞ = –7º) and the temperature ($T_{H\infty}$ = 8000–12000 K) inside the heliosphere (Bertaux et al., 1985; Ajello et al., 1994; Lallement, 1996; Clarke et al., 1998; Quemerais et al., 1994, 1999; Costa et al., 1999). The most recent determination of the parameters for hydrogen using hydrogen absorption cells have been reported by Lallement et al. (2005) where $v_{H\infty}$ = 22 ± 1 km/s, $T_{H\infty}$ = 11500 ± 1000 K, λ_∞ = 72.5±0.5º and β_∞ = –8.8±0.5º are found. The flow direction of the interstellar H inside the heliosphere is offset from that of He by 4±1° (Lallement et al., 2005) and close to the velocity vector of the local interstellar cloud, λ_{LIC} = 74.5º and β_{LIC} = –7.8º, as observed by HST (Lallement, 1996). The observed difference between the H and He flow direction in the inner heliosphere is probably due to the deflection of interstellar plasma by the interstellar magnetic field and the strong neutral gas plasma interaction of hydrogen. In this connection it should be noted that potential experimental evidence for a second, more energetic, neutral particle stream possibly related to the interstellar gas has been presented (Collier et al., 2004; Wurz et al., 2004). However, its interpretation is still rather controversial, and improved observations are needed to test the hypothesis of such a second stream.

As a consequence of the interaction with the plasma H is also substantially filtered at the heliospheric boundary. Therefore, the density outside the heliosphere has to be inferred through modeling. Pickup ion observations (discussed in more detail in Section 8.2.4) provide an estimate for the hydrogen density at the termination shock of $n_{H,TS}$ = 0.095±0.01 cm^{-3} (Gloeckler and Geiss, 2004), which agrees well with $n_{H,TS}$ = 0.09±0.02 cm^{-3} as derived from the slowdown of the solar wind through mass loading with H^+ pickup ions (Wang and Richardson, 2003). Combining the measured ISN H density inside the heliosphere with a pressure balance between solar wind and ISM and using a kinetic model for the filtration, Izmodenov et al. (1999, 2004) deduced a neutral H density $n_{H,ISM}$ = 0.18 cm^{-3} and a proton density n_{H^+ISM} = 0.06 cm^{-3} for the local ISM. UV instrumentation is also part of the Pioneer and Voyager spacecraft. These observations provide insight into the interstellar neutrals at larger distances from the Sun and have been used to infer H

and H^+ densities in the surrounding ISM (Gangopadhyay et al., 2002; 2004). In their most recent work, which includes a Monte Carlo radiative transfer model and a global heliosphere model (Baranov and Malama, 1993), Gangopadhyay et al. (2004) report a neutral density $n_{H,ISM}$ = 0.15 cm^{-3} and a fraction of ionized hydrogen $n_p/(n_p + n_{H,ISM}) = 0.3$. Their best fit to the UV data for the H density at the termination shock suggests 0.08 cm^{-3}. Considering the rather difficult absolute calibrations for UV observations, these results are in good agreement with the values derived from the in situ particle observations. The results imply that only $\approx$50% of the H atoms pass through the heliospheric boundary.

8.2.3 Neutral Solar Wind

Neutral solar wind (NSW) originates from solar wind ions, which become neutralized during their travel from the Sun through interplanetary space. Consequently, NSW moves in the anti-Sunward direction with solar wind velocity, i.e., 300–800 km s^{-1}. The mechanisms suggested for the creation of NSW are charge exchange with neutral gas (e.g. the inflowing interstellar gas or the exosphere of a planet) or interaction of solar wind ions with interplanetary dust particles. The dominant portion of dust particles stems from the fragmentation of comets and asteroids. Kuiper belt dust and interstellar dust are only a small fraction of the dust population in the inner heliosphere (Mann et al., 2004). In addition, it has been speculated that neutral atoms in the solar wind could originate directly from ejections of solar matter (Akasofu 1964a,b; Illing and Hildner, 1994). Fahr (1968b) suggested that charge exchange between solar protons and neutral hydrogen near the Sun would create NSW that would penetrate into the Earth's thermosphere and could raise the temperature and density. Holzer (1977) examined the consequences of interplanetary atomic H on the solar wind and concluded that charge transfer would produce a NSW fraction of $3 \cdot 10^{-5}$ at 1 AU. Gruntman (1994) estimated the NSW fraction observed near Earth as 10^{-5}–10^{-4}, depending on the time of the year. Such small fractions have a negligible effect on the Earth's upper atmosphere (Yeghikyan and Fahr, 2004).

The charge exchange process between an ISN atom, A_{ISN}, and a solar wind ion, B^+_{SW}, is described as

$$A_{ISN} + B^+_{SW} \xrightarrow[\sigma_{CE}]{} A^+_{ISN} + B_{SW} \tag{8.8}$$

with a charge exchange cross section σ_{CE}. The resulting ion A^{+}_{ISN} is a newly created pickup ion, and B_{SW} is a NSW atom. Typically one electron is exchanged between the collision partners, which means that NSW created by this process will be composed almost entirely of H. The most important charge exchange processes occur between H and solar wind protons,

$$H_{ISN} + H^{+}_{SW} \xrightarrow[\sigma_{CE}]{} H^{+}_{ISN} + H_{SW} \tag{8.8a}$$

with a cross section $\sigma_{CE} = 1.7 \bullet 10^{-15}\ \mathrm{cm}^2$ (Maher and Tinsley, 1977), and between He and solar wind alpha particles

$$He_{ISN} + He^{++}_{SW} \xrightarrow[\sigma_{CE}]{} He^{++}_{ISN} + He_{SW} \tag{8.8b}$$

with a cross section $\sigma_{CE} = 2.4 \bullet 10^{-16}\ \mathrm{cm}^2$ (Barnett et al., 1990). The highly charged heavy ions (e.g. C^{5+}, O^{6+} or Fe^{10+}) may reduce their charge states as a result of collisions with neutral gas atoms, but will not end up as neutral atoms. The total NSW flux Φ^{ISN}_{NSW} from charge exchange with the ISN gas is derived by integrating this process from the Sun to the location of the observer.

$$\Phi^{ISN}_{NSW}(r,\theta) = \int_0^r n_{SW} \left(\frac{r_E}{r'} \right)^2 v_{SW}\, \sigma_{CE}\, n_{ISN}(r',\theta)\, dr' \tag{8.9}$$

n_{SW} is the solar wind density at r_E = 1 AU, which scales quadratically with distance from the Sun. With the interstellar gas density from Eq. 8.3 this yields

$$\begin{aligned} \Phi^{ISN}_{NSW}(r,\theta) &= n_{SW} v_{SW} \frac{\sigma_{CE}\, v_{ISN}}{\beta_A} \frac{\sin\theta}{\theta} n_{\infty} \exp\left(-\frac{\beta_A\, r_E^{\,2}}{v_{ISN}\, r} \frac{\theta}{\sin\theta} \right) \\ &= n_{SW} v_{SW} \frac{\sigma_{CE}\, v_{ISN}}{\beta_A} \frac{\sin\theta}{\theta} n(r,\theta) \end{aligned} \tag{8.10}$$

Neutralization of solar wind ions by dust in the inner heliosphere can occur through two processes. Firstly, solar wind ions are implanted into the dust grains, saturate the outer layer with gas over time, and are released later via natural outgassing of the dust particle (Banks, 1971; Fahr et al., 1981). Similarly, atoms and a small fraction of ions are released

from the surface of dust particles into space through sputtering by impinging solar wind ions. Fortuitously, the solar wind energy is about 1 keV/nuc, which is about the energy for the maximum sputter yield, and the total sputter yield of solar wind is approximately 0.15 atoms per incident ion, assuming a typical mix of solar wind ion species. The sputtered neutrals and ions contribute material from the dust grains to the environment. Together, these processes establish a neutral gas source close to the Sun that results in the charge exchange reactions as described by Eq. 8.8. Fahr et al. (1981) calculated that dust-generated neutral H dominates over ISM H inside 0.5 AU. NSW created in this way, again, will be mostly H. In a second process solar wind ions traverse sufficiently small dust particles and emerge with a lower charge state or even neutralized (Collier et al., 2003; Wimmer-Schweingruber and Bochsler, 2003). With typical energies of 1 keV/nuc solar wind ions will penetrate dust grains in the size range 100 to 300 Å or the corresponding range at the edge of larger grains. The second process also allows for NSW atoms other than H. However, upon traversal through a dust grain the particles will lose a substantial fraction of their energy, and part of the resulting NSW will be significantly slower than the ionized solar wind. Ions that are generated out of the dust-generated neutral gas and the sputtered ions are referred to as "inner source" pickup ions (Geiss et al., 1996). Therefore, also solar wind ions that have assumed a low charge state and end up with very low speed after penetration of dust grains may contribute to the "inner source" ions (Wimmer-Schweingruber and Bochsler, 2003).

NSW produced by dust via the first process is given by Banks (1971)

$$\Phi_{NSW}^{dust,1}(r) = \frac{\sigma_{CE} \cdot (n_{SW} v_{SW})^2}{\beta} r_E \Omega_1 \left(\frac{r_E}{r} \right)^2 \ln\left(\frac{r}{r_{\min}} \right) \tag{8.11}$$

where Ω_1 is the total integrated cross-section of the dust from the Sun to the observer located at r_E and β is the rate for charge exchange between solar wind ions and dust-generated neutral gas at 1 AU. For small distances, Ω_1 can be imagined as the probability per unit length that a particle will be absorbed by dust.

$$\Omega_1 = \int_{s_{\min}}^{s_{\max}} f(s,r)\, \pi s^2\, ds \tag{8.12}$$

Equation 8.12 represents the integral over the entire size distribution $f(s,r)$ of dust particles of size s, assuming spherical dust grains (Banks, 1971), where *f(s,r)ds* is the local number density of dust grains. For simplicity, a size distribution $f(s,r) = f_E(s) \bullet (r_E / r)$ is assumed, which does not vary in shape, but whose density falls off linearly with distance from the Sun, as is considered valid outside $0.1\ r_E$ (Mann et al., 2004). Previously, radial dependencies were reported that are close to linear: $(r_E/r)^{1.25}$ (Levasseur et al., 1991) and $(r_E/r)^{1.3}$ (Richter et al., 1982). Note that the solar wind flux enters as a quadratic term in Eq. 8.11, because dust particles are saturated with solar wind and thus the outgassing neutral gas flux is also proportional to the solar wind flux into the particle. In addition, there is an inverse quadratic radial dependence that confines this process close to the Sun.

NSW that arises from interaction with dust via the second process is given by

$$\Phi_{NSW}^{dust,2}(r) = p_0\, n_{SW}\, v_{SW} r_E\, \Omega_2 \left(\frac{r_E}{r} \right)^3 \tag{8.13}$$

with p_0 being the probability that the emerging particle is neutral and Ω_2 the integrated cross-section for the dust penetration process at r_E. The cubic radial dependence in Eq. 8.13 is a combination of the quadratic solar wind flux decrease and the linear dust density decrease with distance from the Sun. Thus, NSW from both processes is created preferentially close to the Sun, with an even stronger concentration for the latter process. The integral of the total dust cross-section, Ω_2, based on this second process may be smaller because the interaction with larger grains is limited to their edge regions, and small dust particles could be depleted close to the Sun because of magnetic and drag forces (e.g. Ragot and Kahler, 2003; Mann et al., 2004). Therefore, the contribution of the second process to the generation of NSW is potentially weaker than that of the first process, and may be solar cycle dependent, but a number of questions still remain to be answered.

It should be emphasized that the dust that contributes to the generation of NSW is solely of interplanetary origin. Although a stream of interstellar dust through the solar system has been detected with Ulysses (Grün et al., 1994), these particles constitute only a small fraction of the

dust in interplanetary space with a very specific velocity distribution. Compared with gas the contribution of dust is already small in the ISM. For typical ISM clouds, gas to dust mass ratios of 100 to 170 are found (e.g. Spitzer, 1978), and more recently a value of 180 ± 3 has been deduced for the local neighborhood of the heliosphere (Frisch et al., 1999; Landgraf, 2000; Frisch and Slavin, 2003). In addition, the small dust grains are strongly filtered by the interplanetary magnetic field (Landgraf et al., 2003). Therefore, the importance of interstellar over interplanetary dust is rather small in the inner heliosphere (Mann et al., 2004). Although during the passage of denser interstellar clouds the relative importance of interstellar dust will increase (Landgraf, this volume), the high gas to dust ratio in the interstellar material will lead to dominant NSW production from the neutral gas component.

NSW created close to the Sun may be ionized again on its way out. The probability of an atom born at distance r_0 from the Sun to reach a point further out in the heliosphere at distance r is

$$p_S(r, r_0) = \exp\left(-\frac{\beta_A {r_E}^2}{v_{SW}} \left(\frac{1}{r_0} - \frac{1}{r} \right) \right) \tag{8.14}$$

Since NSW propagates with the solar wind speed, the relative velocity between solar wind ions and NSW is close to zero and the probability for charge exchange is negligible (see Eq. 8.1). In addition, this would not change the NSW flux, since two co-moving particles would exchange their charges. However, NSW may still be photo-ionized, but these rates are lower than the charge exchange rates between ISM H and solar wind (Rucinski et al., 1996) and NSW travels at solar wind speed, much faster than ISN. Thus most of the NSW will escape into the interplanetary medium. Only NSW created inside ≈ 0.5 AU will be noticeably affected.

Observational evidence of NSW thus far is very scarce because of the difficulty in measuring neutral particle fluxes several orders of magnitude lower than the solar wind flux, while simultaneously being exposed to full sunlight. The only observation thus far was made with LENA on IMAGE, from which a NSW fraction of ~10^{-4} was derived (Collier et al., 2001). Enhancements in the NSW flux due to charge exchange in the geocorona were observed, with the NSW fraction increasing to a few times 10^{-4} (Collier et al., 2001). Since the NSW fraction outside the geocorona was found to be roughly constant along the Earth's orbit for large intervals, it was concluded that the neutralizing agent cannot be the ISN

gas flow (Collier et al., 2003), which should have a pronounced seasonal modulation (Bzowski et al., 1996). Only in the upwind direction will charge exchange with the ISN gas give a NSW fraction of ~10^{-4} (Wurz et al., 2004). Therefore, interaction with dust was suggested, which is distributed evenly in the inner heliosphere (Richter et al., 1982). From the observed NSW fluxes the total dust cross section was determined to be $\Omega < 6 \bullet 10^{19}$ cm ^{1} at 1 AU (Collier et al., 2003).

Obviously under current conditions NSW is mainly generated by interplanetary dust, because the fluxes of ISN gas into and the available gas densities in the inner heliosphere are very small. Therefore, the production of NSW by charge exchange is insignificant when evaluated for effects on planetary atmospheres. If the ISN velocity were substantially increased and/or the ISN gas density were much higher, a NSW fraction in the range of a few percent, or even beyond, may result as will be discussed below.

8.2.4 Pickup Ions

Through charge exchange with the solar wind, which also produces NSW, as well as through photo and electron impact ionization pickup ions are generated out of the neutral interstellar gas. These pickup ions constitute an important component of the interplanetary plasma population throughout the heliosphere. They were first detected for He in 1984 (Möbius et al., 1985) and for H in the 1990's (Gloeckler et al., 1993). Because the interstellar gas flow is slow compared with the solar wind, the initial velocity at ionization, which equals the neutral gas velocity, is usually neglected and pickup ions are modeled starting with $v = 0$. In the solar wind frame, they are injected with negative solar wind velocity $-v_{SW}$, which leads to a gyration about, and motion along, the interplanetary magnetic field, with the perpendicular and parallel component of the injection velocity distributed according to the orientation of the interplanetary magnetic field (IMF). In velocity space seen in the solar wind frame, the initial distribution of pickup ions in polar coordinates is $f_i(\mathbf{v}) = f_0 \delta(v \quad v_{SW}) \delta(\theta \quad \theta_o)$, where θ_o is the initial pitch angle of the pickup ions, which is equal to the angle of the IMF relative to the solar wind.

In the standard picture, pitch angle scattering due to Alfvén waves embedded in the IMF redistributes the pickup ions into a spherical shell in velocity space, and subsequently the shell shrinks due to adiabatic

cooling during the radial expansion of the solar wind (e.g. Vasyliunas and Siscoe, 1976; Möbius et al., 1988). Observations have shown that the pickup ion distribution very often deviates drastically from this simple spherically symmetric shape due to inefficient pitch angle scattering (Gloeckler et al., 1995; Möbius et al., 1998; Oka et al., 2002) and that their flux and spectra are highly variable in space and time (Gloeckler et al., 1994; Schwadron et al., 1999; Saul et al., 2003). However, in order to evaluate the large-scale contribution to the particle population in the inner heliosphere by particles produced out of the interstellar gas flow, we can safely integrate over such variations and thus neglect them, as has been successfully done for the determination of the local interstellar parameters from pickup ions (Gloeckler et al., 1996; Gloeckler and Geiss, 2001; Gloeckler et al., 2004; Möbius et al., 2004). In this standard view the pickup ion distribution function $f(v)$ describes their production along the spacecraft-Sun line by

$$f(v)4\pi v^2 dv = n_{ISN}(r)\cdot\beta_A dt \tag{8.15}$$

Assuming adiabatic cooling of the pickup ions in the solar wind like an ideal gas and using the fact that both the pickup ion density of already accumulated ions and the ionization rate decrease as $1/r^2$ with distance from the Sun, the relation

$$f(v) = \frac{3n_{ISN}(r)\cdot\beta_A\cdot r_{obs}}{8\pi\, v_{SW}^4}\left(\frac{v}{v_{SW}}\right)^{-3/2} \tag{8.16}$$

emerges for the interstellar pickup ion distribution. In this relation β_A represents the ionization rate at the location of the observer. Recognizing that

$$r = r_{obs}\cdot\left(\frac{v}{v_{SW}}\right)^{3/2} \tag{8.17}$$

describes the radial dependence of the adiabatic cooling, $f(v)$ represents a mapping of the radial distribution $n_{ISN}(r)$ of the interstellar neutrals inside the observer location into the observed velocity distribution of the pickup ions.

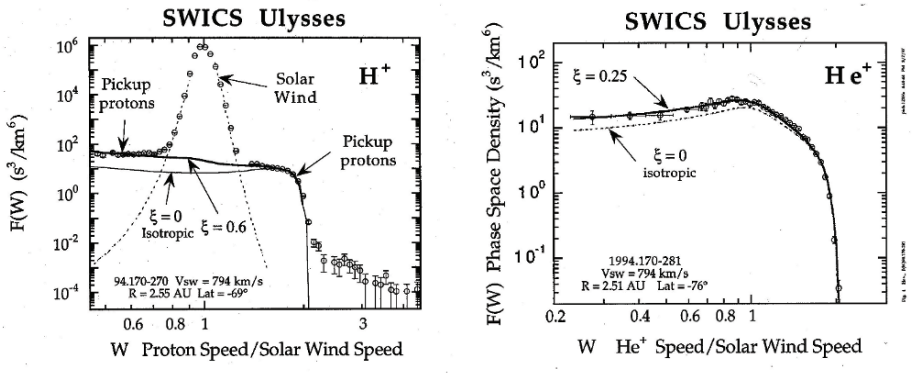

Figure 8.2. Phase space density spectra of H^+ (left) and He^+ (right) pickup ions (Gloeckler and Geiss, 1998). The H^+ distribution includes a suprathermal tail above $W > 2$, which is invisible for He^+, because the dynamic range in this plot is more limited.

Figure 8.2 shows energy spectra of the pickup ion phase space density for H and He (Gloeckler and Geiss, 1998). Here the observations are shown as a function of the ratio W of the pickup ion speed v to the solar wind speed v_{SW} to be able to integrate over times of varying solar wind speeds. The phase space density spectrum of H^+ pickup ions appears much flatter than that of He^+ between $1 < W < 2$, which reflects the fact that the H ISM density falls off much faster towards the Sun than that of He. Observations of the He^+ spectra over the course of one year in Earth's orbit, or at the Lagrange point L1, contain the distinct longitudinal structure of the He focusing cone (Möbius et al., 1995; Gloeckler et al., 2004), as can be seen in Fig. 8.3, which shows a combination of data from the 1980's with AMPTE SULEICA and data obtained after 1997 with ACE SWICS. The substantial variation of the cone, with maximum height during solar activity minima around 1985 and 1997 and reduced height during solar maximum, becomes obvious. The prominence of the He cone as the most important spatial feature of the interstellar gas flow through the inner heliosphere is a combined function of ionization rate, interstellar flow speed and temperature (Fahr et al., 1979; Wu and Judge, 1979) and thus depends on solar and interstellar conditions.

The knowledge of the radial distribution of the neutrals and the local ionization rate are sufficient to calculate the pickup ion velocity distribution and their absolute density. Under current conditions He^+ pickup ions make up $\approx 8 \cdot 10^{-4}$ of the solar wind He flux at 1 AU outside the focusing cone and $\approx (4–8) \cdot 10^{-3}$ in the cone center, depending on the solar cycle phase. Compared with the bulk solar wind density, this fraction is a

factor of ≈16 lower, because the average abundance of He^{2+} is ≈6% in the solar wind. Therefore, pickup ions at 1 AU constitute a mere test particle population in interplanetary space. While interstellar He is present deep inside Earth's orbit and dominates the pickup ion population at 1 AU, the main component of the ISM, hydrogen, is noticeable only outside ≈3 AU. Dust-related "inner source" pickup ions dominate close to the Sun (Gloeckler et al., 2000). Because the dust population falls off rapidly with distance from the Sun as discussed above, the inner source pickup ion velocity distribution is already strongly cooled at 1 AU and will continue to do so at larger distances. As the solar wind accumulates interstellar pickup ions on its way outward from the Sun, they become increasingly more important at larger distances. Because interstellar pickup ions are continually injected into the solar wind even at large distances, they form a genuinely hot population and thus dominate the kinetic pressure in the solar wind outside ≈30 AU. Here they lead to so-called pressure balance structures (Burlaga et al., 1996). Outside these distances the implantation of pickup ions also leads to a slowdown of the solar wind due to mass-loading (Richardson et al., 1995; Wang and Richardson, 2003) and substantial pressure modifications (Fahr and Rucinski, 1999, 2001). An extensive review of mass-loading and its effects is given by Szegö et al. (2000). Still, a substantial reduction in solar wind speed due to the accumulation of pickup ions is not felt until close to the solar wind termination shock. In this chapter we will restrict ourselves to effects of the ISM neutrals and related secondaries in the inner heliosphere, while the bulk interaction that leads to the termination of the solar wind is described in the chapter by Zank et al. (this volume).

8.2.5 Singly Ionized Energetic Ions

Over the past decade it has become evident that interstellar pickup ions are a formidable source population for energetic particles in the heliosphere. The initially puzzling observation of a substantial fraction of He^+ in interplanetary energetic ion populations by Hovestadt et al. (1984a), has found its natural explanation with the detection of interstellar pickup He^+ in the solar wind (Möbius et al., 1985). Gloeckler et al. (1994) have identified interstellar pickup He^+ as the main constituent of energetic He ions at energies up to 60 keV in a CIR at 4.5 AU. At 1 AU He^+ also contributes substantially to the suprathermal (up to 300 keV)

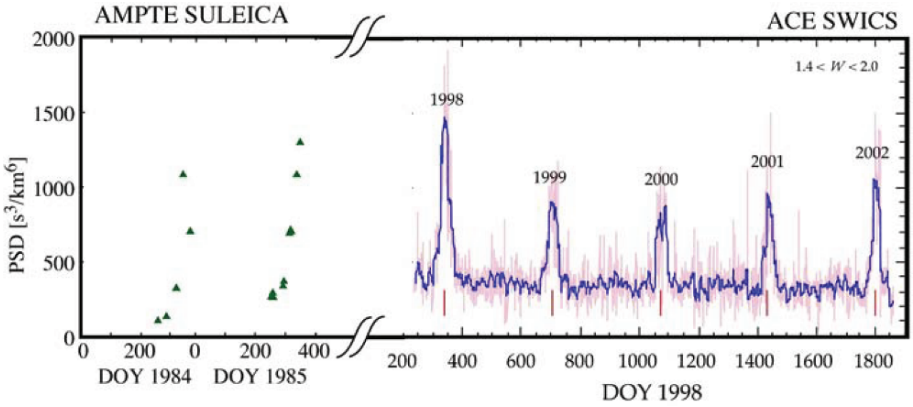

Figure 8.3. Helium focusing cone as seen in pickup ions (adapted from Gloeckler et al., 2004) as observed with AMPTE SULEICA (left) and ACE SWICS (right). The SULEICA data are selected 8–10 hour averages when the satellite was in the solar wind. The SWICS data are shown as 1-day averages (pink) and 10-day sliding averages (blue), indicating the strong intrinsic pickup ion variability.

He population in CIRs (Hilchenbach et al., 1999; Chotoo et al., 2000). Möbius et al. (2002) confirmed this result for more energetic ions (0.25– 0.8 MeV/n) and showed that also interstellar Ne^{+} is present in CIRs. Yet, with $He^{+}/He^{2+} \approx 0.25$, He^{+} is substantially less abundant at 1 AU than in CIRs at 4–5 AU with its dominance over He^{2+}. Moreover, Morris et al. (2001) demonstrated that the He^{+}/He^{2+} ratio increases as the observing spacecraft is magnetically connected to the CIR at increasing distances from the Sun, when the CIR structure sweeps across the observer due to the Sun's rotation. The observed increase of the energetic He^{+}/He^{2+} ratio with time, and thus with distance to the CIR along the magnetic field line, reflects the increasing importance of interstellar He as source material with increasing distance from the Sun.

These results have led to the suggestion that pickup ions are an important source of ions, which can be accelerated very efficiently at interplanetary shocks (Gloeckler, 1999). In a survey of the abundance of He^{+} and He^{2+} (shown in Fig. 8.4) Kucharek et al. (2003) have demonstrated that He^{+} is in fact the third most abundant species in the energetic ion population in the inner heliosphere, after H^{+} and He^{2+}, with $He^{+}/He^{2+} \approx 0.06$ and $He^{2+}/H^{+} \approx 0.03$ (Hovestadt et al., 1984b). Over and above this average ratio, He^{+} is substantially enhanced in CIRs as well as at interplanetary shocks. Bamert et al. (2002) and Kucharek et al. (2003) show that the overwhelming majority of the He^{+} accelerated at these shocks

cannot stem from cold prominence material, even in associated CMEs, since the substantial enhancement in the energetic population occurs outside the region that contains He^+ in the solar wind. Generally, the He^+/He^{2+} ratio is substantially (by a factor of 50–200) enhanced in the energetic ion population (0.25 – 0.8 MeV/n) over its value in the source population, represented by the ratio of pickup He^+ over solar wind He^{2+}. Based on the observed increased efficiency of pickup ions to be injected into the process for acceleration to higher energies, Gloeckler (1999) has argued that the "inner source" of pickup ions may also contribute substantially to the energetic particle population in CIRs. However, in the same study that revealed interstellar He^+ and Ne^+ in the energetic CIR population, Möbius et al. (2002) did not find any evidence for the singly charged C, O, or Mg, expected from the inner source.

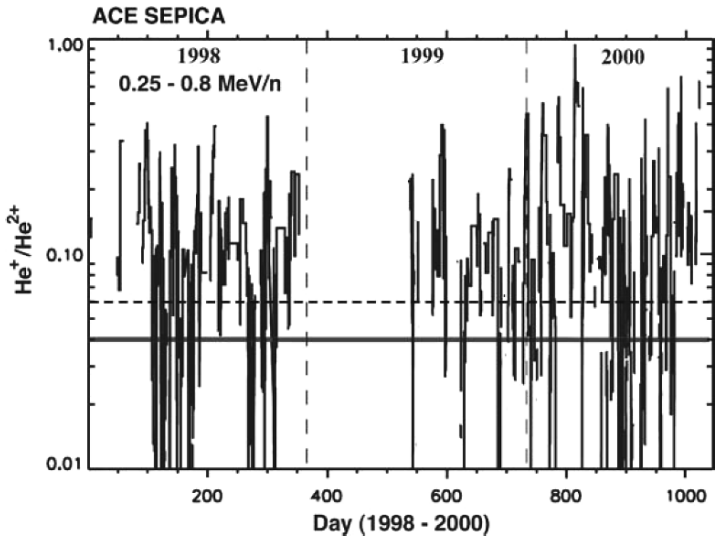

Figure 8.4. Survey of the He^+/He^{2+} ratio in energetic particles for the years 1998 to 2000. An average of 0.06 (indicated by the dashed line) is found with a large variability with values up to 1. The full line indicates the detection limit for He^+ in each individual sampling interval that is determined by a fixed number of He counts.

Because of their advantage in the injection/acceleration process, interstellar pickup ions are a major source of energetic particles in the inner solar system under the current conditions, and their relative importance increases with distance from the Sun. If the density of the neutral gas in the inner heliosphere is boosted by an increased inflow of interstellar gas, both pickup ion density and the abundance of singly-charged

energetic ions will increase accordingly. Such an increase is likely to continue approximately linearly with the increase in the neutral gas density. This increase may be reduced or stopped when mass-loading of the solar wind leads to a substantial slowdown and thus a decrease in the free energy that is available for acceleration and/or when the further acceleration of pickup ions consumes a substantial fraction of the total kinetic energy of the solar wind.

In their interaction with the interstellar neutral gas flow, the suprathermal and energetic particle populations in the heliosphere also generate energetic neutral atoms (ENAs). Gruntman et al. (2001) have shown that the most important source of such ENAs are the energetic particles that are accelerated at the termination shock and the heated solar wind distribution in the heliosheath. As all the ENA populations will roughly scale linearly with the generating ISN density it can be expected that the ENAs from the outer heliosphere remain the dominant contributors also under a wide variety of heliospheric conditions.

8.3 Interstellar Neutral Gas and its Secondary Products under Varying Interstellar Conditions

After discussing the interstellar particle populations in the inner heliosphere, as they are observed in our contemporary heliosphere, we want to set up a grid of models with modified ISM conditions for the discussion of all related modifications in the heliosphere. The size and shape of the heliosphere and thus the related inventory of interstellar neutral gas in the heliosphere react to changes of the total H density, the ionization degree, as well as the ISM temperature and relative velocity. In addition, the heliosphere reacts also to the interstellar magnetic field and cosmic ray environment, but these parameters will influence mainly the influx of cosmic rays into the heliosphere. We will concentrate our discussion in this chapter on substantial changes in the interstellar neutral gas inventory, and we will discuss the consequences for the solar wind, the production of secondary products of the interstellar neutrals, and their influence on the energetic particle populations. However, we neglect the potential subtle modifications of the neutral gas flow due to magnetic field related variations in the interaction between the neutrals and plasma at the heliospheric interface.

A systematic variation of all four relevant parameters would lead to a four-dimensional matrix of cases to be modeled, with an unrealistic amount of effort. However, some of the parameters are linked in their variations in realistic interstellar cloud environments, and not all parameter combinations provide conditions that allow neutral gas influx into the heliosphere. Therefore, we have limited our evaluation to a meaningful subset of cases that we have modeled and that we will discuss in the following sections. The parameter combinations for these cases are compiled in Table 8.1 together with a few descriptive remarks concerning the importance of the choice. Of course, the heliosphere under contemporary conditions is used as a baseline (case 1 in Table 8.1). It is immediately obvious that a variation in the ISM density plays a major role, both for the size of the heliosphere and the resulting densities in the inner heliosphere. Because the effects on the Earth's environment under more drastic changes, when the Earth is either in the outer heliosphere or even outside its boundary, are described in contributions by Zank et al. (this volume) and Fahr et al. (this volume), we restrict the discussion in this chapter to a parameter range for which the termination shock stays at 10 AU, i.e., the Earth remains in the inner heliosphere. As we shall see in the next section, the limiting total density of the ISM under this restriction is $\approx$15 cm $^{-3}$ (featured as case 6). With the reasonable assumption of cosmic abundance for He this brings the maximum He density to $n_{\mathrm{He}} = 1.5\ \mathrm{cm}^{-3}$.

Via the ram pressure balance, the ISM velocity also controls the size of the heliosphere. In connection with the pertinent ionization rate the velocity determines the radial density profile of the neutral gas in the inner heliosphere according to Eq 8.4. As a reasonable range for the velocity of the solar system relative to the ISM, half and twice the current velocity are chosen as bounding values for our discussion. This covers a typical range of peculiar velocities for so-called intermediate velocity gas clouds in the solar neighborhood (Welty et al., 1999). For H the full range of velocities is explored for the current warm ISM (cases 1–3) and only the high-velocity case for a cold ISM cloud with current density (case 4). High ram pressure situations are added for cold and dense clouds with cases 6 and 7. The focusing cone of He is determined by a combination of the ISN velocity and temperature. Therefore, He is modeled with all velocities for the current temperature and for a cold cloud of 10 K (cases 1–6), while the main variations for H are covered with only

two velocities at 10 K. For He the density distribution is modeled relative to the density in the ISM, and the He distributions can be scaled linearly to any density value. Therefore, the density values given in Table 8.1 are only relevant for H. It should be noted that dense interstellar clouds are usually cold and that they have most likely a rather low fractional ionization, with no need of individual variation of these parameters. For H we capitalize on the availability of model heliospheres calculated in the chapter by Zank et al. (this volume) instead of modeling all of our cases listed in Table 8.1. As a trade-off, we incur a slight temperature mismatch for cases 1–3, where we use a LISM H temperature of 7000 K instead of 6000 K for cases 1 and 3, and an H temperature of 3000 K for the low-speed case 2. As these cases have a supersonic LISM, the consequences of temperature deviations, both for the morphology and especially for the neutral hydrogen content in the inner heliosphere, are negligible, and the H models 1–3 presented in detail below are good proxies for the cases 1–3 in Table 8.1. Finally, the case of the hot local bubble environment (case 8) has only been included for completeness, as the almost full ionization precludes the penetration of neutral interstellar gas into the heliosphere. Thus no modeling of the He was performed for this case.

Table 8.1. Environmental conditions for the heliospheric models.

Case #	n_H (cm^{-3})	n_H^+/n_H	T (K)	v_{ISN} (km/s)	Species	Comments
1	0.26	0.18	6000	26	H, He	Contemporary heliosphere
2	0.28	0.14	6000	13	H, He	Warm cloud, different speed
3	0.24	0.42	6000	52	H, He	Warm cloud, different speed
4	0.28	0.14	10	52	H, He	Cold cloud, high speed
5	0.28	0.14	10	13	He	Cold cloud, different speed
6	15	0.01	10	26	H, He	Cold and very dense cloud; He density scales
7	1	0.04	10	52	H	Fast, cold, and dense cloud
8	0.005	1	$1.25 \cdot 10^6$	13	H	Hot bubble; no He inflow

8.3.1 Variation of the interstellar H distribution in the inner solar system

An overview of the ISN gas distributions in the heliosphere and their modeling has been given in Section 8.2.1. It is important to note here that the mean-free-path for charge exchange is mostly larger than typical heliospheric distances, so that neutral H is in effect not in equilibrium in

and around the heliosphere. This holds for interstellar environments over a range of different densities up to at least ten times the current ISM density, because the size of the heliosphere varies with the density of the surrounding medium. Therefore, models of neutral H throughout the heliosphere tend to be complex and need to account at least for the behavior of each of the different neutral gas components. Following in detail the evolution of all the neutral populations in space, energy, and time, would call for a full kinetic treatment of the neutral component (e.g. Baranov and Malama, 1993; Izmodenov et al., 2001), which is very computer intensive. An alternate, computationally less expensive approach, which captures the spatial distribution of the neutral gas flow throughout the heliosphere with sufficient accuracy for the purpose of this discussion, is to approximate the neutral distribution with multiple fluids. Therefore, the modeling used in this section draws from a three-fluid approach by Zank et al. (1996). In this model the neutral hydrogen of the ISM (either flowing in from afar or born outside the heliopause) is labeled component 1 (fluid one), neutral H born through charge exchange in the hot heliosheath is labeled component 2, and neutral H products created by charge exchange in the supersonic solar wind (i.e., upstream of the termination shock) are labeled component 3. Component 2 neutrals have a very hot distribution with a mean velocity of ~100 km/s as they are characterized by the underlying million degree heliosheath plasma. Component 3 neutrals are cold and fast, and represent the NSW that is generated in the interaction with the incoming interstellar neutrals. The NSW contribution created by dust interactions is not included in this model, as it does not contain any dust component. However, the dust related NSW is not important in most of our model cases, except for the hot Local Bubble (case 8), when no interstellar neutrals reach the inner heliosphere.

The balance between solar wind ram pressure and interstellar pressure determines the size and shape of the heliosphere. The termination shock distance can be calculated according to:

$$r_{TS} = C\sqrt{P_{1AU} / P_{ISM}} \tag{8.18}$$

where $P_{1AU} \approx \rho_{1AU} v_{SW}^2$ is the solar wind ram pressure at 1 AU. Similarly the total ISM pressure is defined as $P_{ISM} \approx m_H n_H v_{ISM}^2 + P_{therm}$, where P_{therm} is the thermal pressure in the surrounding ISM. The constant C in Eq. 8.18 is of order 1 AU following Zank et al. (this volume). Assuming

an unchanging solar wind pressure, it can be expected from pressure balance that the distances to the termination shock and heliopause, respectively, scale inversely with the interstellar velocity, and inversely with the square root of the interstellar density.

For cases 1–7 in Table 8.1 the pressure balance is dominated by interstellar ram pressure, whereas for case 8 the ISM is subsonic and thermal pressure takes over. Case 8 represents the era (thought to be several million years ago) when the Sun was in the interior of the so-called Local Bubble, a hot, tenuous ISM (Frisch and Slavin, this volume). This scenario provides for a relatively uninteresting picture. A total density $n_\infty = 5 \cdot 10^{-3}$ cm^{-3} and a temperature of $T_\infty = 1.25 \cdot 10^6$ K surprisingly lead to a heliosphere of similar size as today. In spite of the much-reduced density the total outside pressure remains comparable to current conditions because of the high temperature. In this case the speed of the Sun relative to the local environment is not even important, because the interaction is strongly subsonic. Therefore, the heliosphere will be axisymmetric along the interstellar magnetic field, unlike today (Parker, 1963).

Because of the high temperature the interstellar medium will be almost fully ionized, and no interstellar neutral gas will enter the solar system. This removes the possibility of creating any significant amount of secondary particle populations inside the heliosphere, such as neutral solar wind, pickup ions, and their more energetic brethren. ACRs will also be almost absent. The generation of any secondary particles will be restricted to the interaction with dust, of interplanetary and interstellar origin, inside the heliosphere. Because the interstellar dust density is typically very low with gas to dust mass ratios of 100 to 170 (Spitzer, 1978) and the total gas density of the ISM is extremely low in case 8, there will be almost no interstellar dust in the heliosphere. Therefore, the amount of dust-related interactions will be controlled completely by the interplanetary dust component and will probably not be much different from what is observed under current conditions for the neutral solar wind (Collier et al., 2001, 2003) and inner-source pickup ions (Geiss et al., 1996; Gloeckler et al., 2000). Under such circumstances there would certainly be no possibility to deduce the surrounding interstellar conditions from in situ observations inside the heliosphere, as is possible today. Astronomers would have to resort solely to remote sensing techniques to obtain just average line-of-sight information about the surrounding medium.

Starting with the contemporary heliosphere (case 1) in the upper left, Figure 8.5 shows four different models, representing a change in interstellar pressure by a factor of 16. It can be seen that both density increases and velocity increases lead to smaller heliospheres. Shown is the plasma temperature in color-coding, which illustrates the location of critical boundaries, such as the termination shock, and significant neutral gas – plasma interaction through increased values. Case 6 represents the smallest heliosphere modeled here, with the upwind termination shock only 8 AU from the Sun and the heliopause at 12 AU. Note that this means that Saturn dips periodically into the hot heliosheath, crossing the termination shock, and Jupiter's orbit goes through regions of heated supersonic solar wind close to the upstream region of the termination shock.

Generally speaking, the morphology of the heliosphere is preserved even in these extreme cases. Going to higher interstellar speeds does however increase the termination shock upwind/downwind asymmetry. Also, the presence of more neutral ISM H inside the termination shock leads to more pickup ion heating, as is evident from the increased plasma temperatures in Figure 8.5.

The amount of interstellar H that penetrates into the heliosphere inside the termination shock is not only a function of the interstellar neutral density at infinity, but also depends on the interstellar velocity. This is evident in the density profiles along the stagnation axis as displayed in the left panel of Figure 8.6, where the red profile corresponds to the contemporary heliosphere. The dark blue curve represents the high-density case 6, the green ones are high-speed cases, and the cyan profile is a low-speed case. Note that the modeled cases can have component 1 neutral densities that are two orders of magnitude higher at 1 AU than in the contemporary configuration. This higher neutral H density naturally results in a higher charge-exchange rate, and the by-products are component 3 neutrals whose densities are shown in the right panel of Figure 8.6. Again, at 1 AU, the absolute NSW densities of case 6 are two orders of magnitude higher than in the contemporary heliosphere. Even in this cold high-density case the neutral H density at 1 AU does not exceed 0.3 cm^{-3} and thus is at least one order of magnitude below the average solar wind density. As we will see below, all secondary products can still be considered as test particles, and they do not contribute significantly to the solar wind dynamics. Even on the upwind side and crosswind, the density of interstellar He is higher by a factor of 3–5 than that of H.

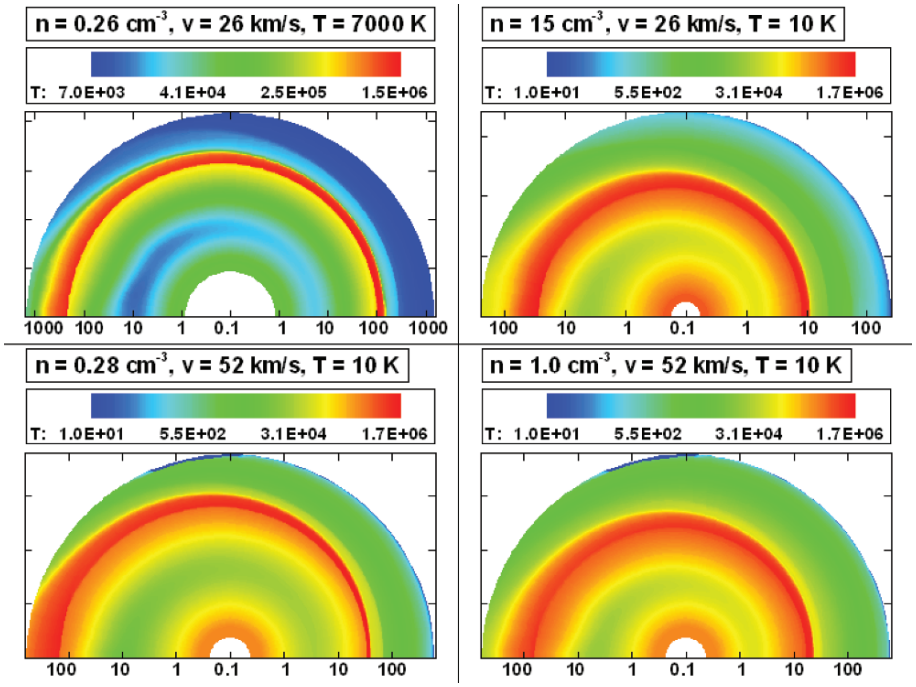

Figure 8.5. Two-dimensional maps of plasma temperature for four different models, counterclockwise from upper left: case 1, case 4, case 7, and case 6. The distance scale is logarithmic in AU, with stagnation axis angle preserved. In each map, the ISM comes in from the right; the first temperature rise is the bow shock, the thin red feature is the heliosheath/heliotail between heliopause and termination shock. The supersonic solar wind is heated by the pickup ions.

8.3.2 Variation of the interstellar He distribution in the inner solar system

Under contemporary conditions He is the dominant interstellar species in the inner solar system, inside approximately 3 AU, because of its rather high ionization potential. It is expected that He will remain the dominant species for all situations with a substantial neutral gas flow through the heliosphere. The density of interstellar helium in the inner heliosphere scales linearly over a wide range with the density of the inflowing gas. Therefore, it will suffice to model the conditions for a single neutral gas density. For total gas densities below $\approx$100 cm^{-3} the gas can be considered collisionless, which allows for a simple scheme with

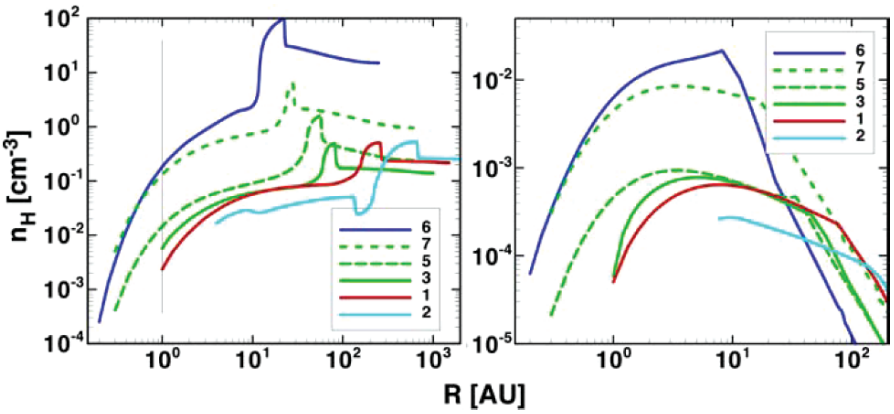

Figure 8.6. Left Panel: Profiles of neutral H density (interstellar + hydrogen wall component), in cm^{-3}, along the upwind stagnation axis, in AU for cases 1–3 and 5–7. The hydrogen walls are evident, as is photo-ionization for small distances from the Sun. Right Panel: Profiles of neutral H component 3 density (i.e., born through charge exchange with the supersonic solar wind), in cm^{-3}, along the upwind stagnation axis.

the atoms following Keplerian trajectories for the calculation of the density and higher moments of its distribution function. We have restricted ourselves to densities even below 15 cm^{-3}, because for densities exceeding this number the Earth will not be in the inner heliosphere, since the termination shock will move inside 10 AU (Fahr et al., Zank et al., this volume).

Because the interplay between the He flow, the Sun's gravitation, and ionization leads to a characteristic focusing cone structure in the inner heliosphere, which depends on the flow velocity and temperature of the gas as well as on the ionization rate, a range of velocities and temperatures need to be explored. We restrict ourselves to typical ionization rates for the contemporary heliosphere (see Rucinski et al., 1996; McMullin et al., 2004) since the emphasis in this book is on the response of the heliosphere to external conditions and not to solar activity. There is no point in calculating a model for a hot interstellar medium with T_∞ = 10^6 K because the medium is almost completely ionized and no noticeable neutral gas flow will reach the inner heliosphere. Calculation of "warm" heliospheres (T_∞ = 6000 K) with different velocities does not differ from the contemporary case since the gas has a thermal character (its thermal velocity is comparable to the bulk speed). For these cases a hot model (Wu and Judge 1979, Fahr 1979) was used.

The calculation of "cold" heliospheres (T_∞ = 10 K, cases 4–6) can in principle be performed with the use of the same model, even the same numerical code. In practice, however, the hot model approach becomes computationally costly because of the extremely narrow peaks of the distribution functions related to the very small thermal spread. Fortuitously, for such a low temperature the analytical cold gas approximation (Axford 1972) can be used except close to the cone center, where the thermal spread of the gas, however small it is, must be taken into account to avoid singularities in the computational scheme around the downwind axis in the cold model.

We are using a stationary model for the He distribution here, although it is known that the temporal variation of the ionization rate influences the spatial He distribution inside the heliosphere. However, this simplified approach is justified because for the discussions in this chapter we are interested in the average and extreme values of the neutral gas densities in the inner heliosphere, and not so much their temporal evolution or their detailed spatial pattern. To illustrate the differences between the contemporary warm interstellar gas environment and a typical cold gas cloud, Figure 8.7 shows a 2-dimensional cut through the He density distribution that includes the cone for a warm and a cold interstellar environment. The color-coding has been adjusted to the corresponding maximum density in the cone for each case and does not have any bearing on absolute densities. Compared is the contemporary heliosphere for interstellar gas with a flow velocity of 26 km/s and a temperature of 6000 K with a fast and cold interstellar gas flow of v_∞ = 52 km/s and T_∞ = 10 K. It is obvious that the fast and cold flow produces an extremely narrow focusing cone that is concentrated along the downwind axis. The inset shows the same density distribution, stretched along the y-axis for better resolution of the cone structure. The full density enhancement is concentrated at much less than 0.1 AU around the cone axis. Otherwise the He distribution is very evenly distributed.

To be more quantitative, Fig. 8.8 shows longitudinal density profiles of the neutral interstellar He density at 1 AU normalized to the He density at infinity for the current conditions (case 1), along with cases 2 and 3 in the upper panel, and for a cold interstellar cloud at T_∞ = 10 K with three different relative velocities (cases 4 – 6) in the lower panel. For the cold cloud conditions with an average ionization rate for He of β_{He} =10^{-7} s^{-1} at 1 AU the density enhancement in the peak of the cone exceeds a

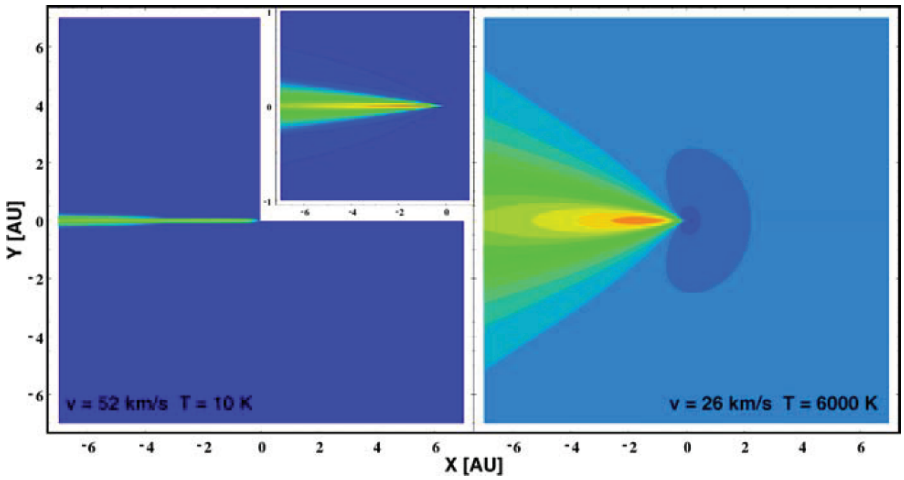

Figure 8.7. Two-dimensional cuts of the neutral interstellar He density distribution in the inner heliosphere in a color-coding based on logarithmic scaling. The colors are adjusted to the maximum density in the cone and do not reflect any absolute calibration. Compared are a contemporary heliosphere (on the right) and a fast cold interstellar gas (on the left). Because of the extremely narrow cone the inset shows a version that is stretched along the y-axis.

factor of 80. Taking the low ionization rate of $\beta_{He} = 6 \cdot 10^{-8}$ s^{-1} at solar minimum, or the high rate of $\beta_{He} = 2 \cdot 10^{-7}$ s^{-1} at solar maximum, the cone is higher by a factor of $\approx$1.5 or lower by a factor of $\approx$3, respectively. In addition, the cones are very concentrated. In order to make the central cone visible for the cold clouds, the angle range is stretched by a factor of 6 in the inset. For the fastest velocity chosen (52 km/s), the cone is extremely narrow, but for 13 km/s the half width of the cone at 1 AU reaches 5^{o}, which is equivalent to almost 0.1 AU, still a substantial width. It should be noted though that even for the highest density in the cone, the mean free path for collisions is $\approx$ 0.25 AU and thus noticeably larger than the cone width. Therefore, the collisionless approximation used in the simulations is still valid. For both 13 and 26 km/s the density enhancement is equal or stronger over the entire angle range as compared with contemporary conditions. Taking into account the increased overall density in the cold dense cloud environment, i.e., $n_{He\infty} = 1.5$ cm^{-3}, the He density will be substantially higher at all locations.

It should be noted that the present interstellar flow vector is inclined about 6^{o} relative to the ecliptic plane (Witte, 2004; Möbius et al., 2004). Therefore, the bulk of such a narrow cone would mostly miss the Earth's

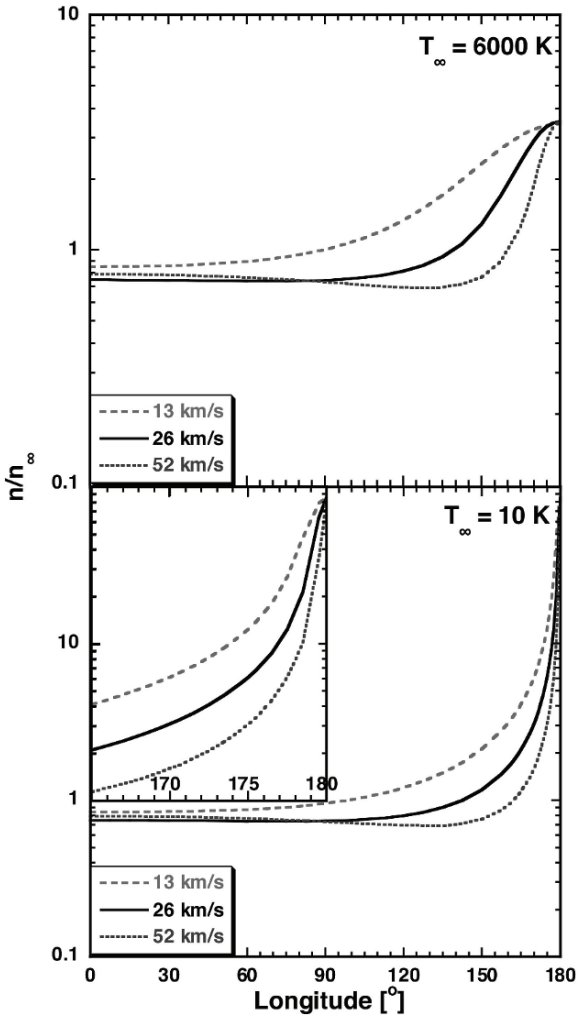

Figure 8.8. Longitudinal density profile of interstellar He at 1 AU exactly across the gravitational focusing cone for ISN gas with T_∞ = 6000 K and 13, 26, and 52 km/s flow, including the contemporary heliosphere (upper panel). Same set of velocities for the cold gas with T_∞ = 10 K (lower panel). Inset: tailward detail of the cold cones (Möbius et al., 2005).

orbit for the current flow direction, and for the majority of interstellar clouds the cone may not directly influence the Earth's environment. If the orientation of the velocity vector were completely random, there is still an $\approx$5% probability for the Earth's orbit cutting through the half-width of the cone for cold conditions with a 13 km/s relative velocity.

8.3.3 Secondary Particles in the Inner Heliosphere

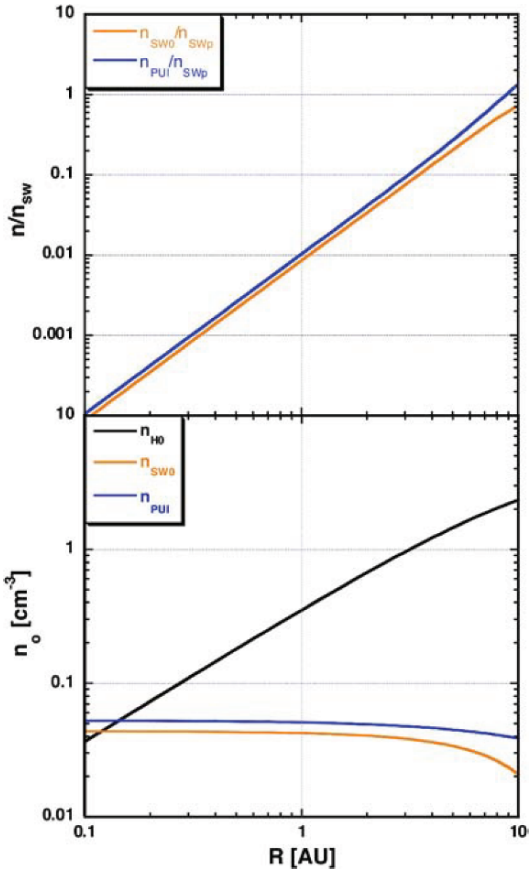

Figure 8.9. Radial variation of the relative contribution of neutral H and pickup H^+ to the solar wind (upper panel) and densities of interstellar H, neutral solar wind H, and pickup H^+ (lower panel, case 6).

Since the density of neutral ISM H remains thinned out substantially in the inner heliosphere, even for dense cold interstellar clouds, the related secondary products, neutral solar wind H, and H^+ pickup ions, constitute a tracer population. Figure 8.9 shows their radial distribution along the upwind axis for the cold and dense ISM (case 6). Since the neutral gas is more depleted in any other direction, it is sufficient for the purpose of this chapter only to consider the upwind direction.

As can be seen from Fig. 8.9, the absolute density of neutral solar wind H, n_{SW0}, and pickup H^+, n_{PUI}, remain below 0.1 cm^{-3} at all distances. Their contribution to the solar wind only becomes substantial

outside 1 AU and is comparable near the termination shock at about 10 AU. At 1 AU both species make up 1% of the solar wind. Although this is substantially more than under current conditions, the solar wind environment will not be changed significantly at Earth's orbit for a cold dense cloud of 15 cm^{-3} H density.

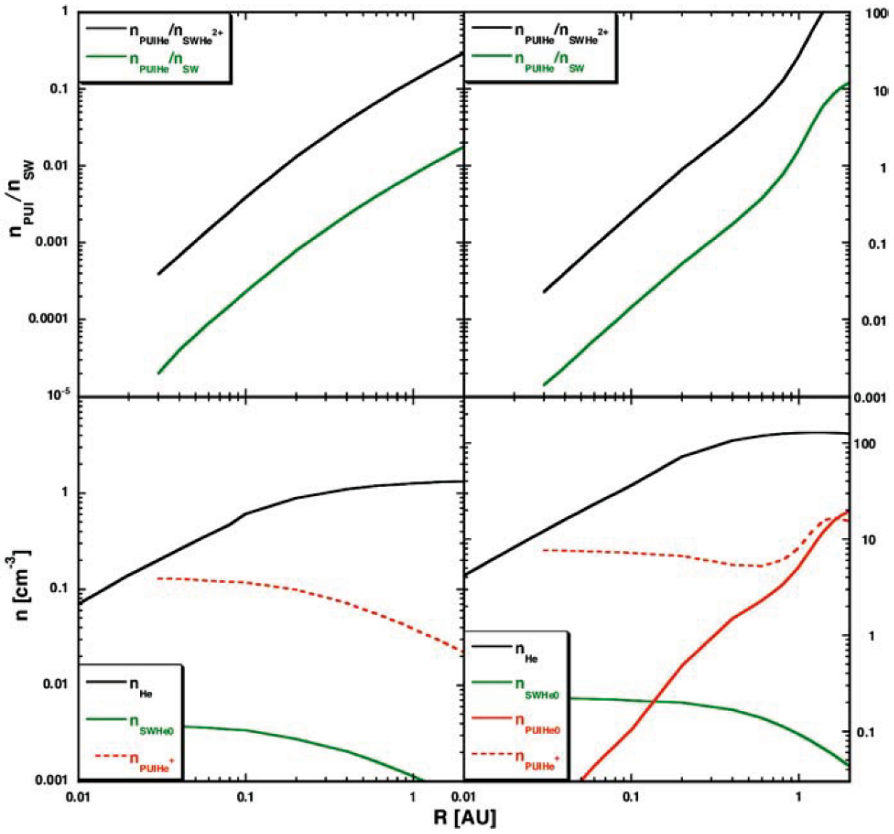

Figure 8.10. Densities of neutral interstellar He (n_{He}), neutral solar wind He (n_{SWHe0}), He^+ pickup ions (n_{PUIHe}+), and pickup ions turned neutrals (n_{PUIHe0}) (lower panels) as well as the density ratio of He^+ pickup ions versus solar wind He^{2+} and H^+ (upper panels) as a function of distance from the Sun (case 5). Upwind is shown on the left and downwind on the right.

As discussed above, neutral He is the dominant interstellar species in the inner heliosphere under all interstellar conditions, and it features the well-known gravitational focusing cone with enhanced density on the

downwind side of the interstellar flow. The dominance of this spatial structure is reflected in the NSW and the pickup ions. Figure 8.10 shows the radial variation of the neutral interstellar He, NSW He, and pickup ion He^+ density in its lower panels. Shown are both radial profiles, along the upwind (left panel) and downwind (right panel) axis. On the downwind side the density of neutrals is also included that stem from charge exchange of pickup ions with the ISN gas. The upper panels contain the fraction of pickup He^+ relative to solar wind protons and alphas. The 13 km/s ISM flow (case 5) has been chosen because it produces the widest cone structure. To compute the secondary products charge exchange cross sections for a 400 km/s solar wind and an average ionization rate of 10^{-7} s^{-1} for He were used. The secondary particles are accumulated starting at 0.03 AU, leaving out the innermost portion of the region where the solar wind is still accelerating and where the neutral densities are negligible. As far as secondary products are concerned, He^+ pickup ions are most important under all circumstances. They exceed the neutral He in the solar wind, typically by a factor of 30, because photoionization is the prevalent production process for He^+ ions (Rucinski et al., 1996; McMullin et al., 2004). NSW hydrogen, produced by the interaction with interstellar He, is even rarer because of the extremely low charge exchange cross section between protons and He, which is lower by about two orders of magnitude compared with double charge exchange between He^{2+} and He. Therefore, NSW hydrogen produced by interstellar He is not even shown here.

Surprisingly, a tertiary neutral particle product becomes very important on the downwind axis. Through charge exchange with the interstellar He neutrals that are strongly enhanced in the cone, He^+ pickup ions, which are also strongly enhanced there, are turned into neutral He with the velocity distribution of the pickup ions. Because the enhancement in the cone translates quadratically into the density of this product, its density is enhanced by about four orders of magnitude compared with the upwind direction. To compute the radial profile of these pickup-ion-generated neutrals, we accumulated their production along the downwind axis, since they also follow the solar wind on average. However, these neutrals will also disperse from the cone region according to their pickup ion inherited velocity distribution. This effect is modeled through a free expansion of the cone structure of these neutrals in two dimensions, using an equivalent thermal speed of the generating pickup ion distribution

according to Burlaga et al. (1996). For simplicity, the density profile across the cone is assumed to be Gaussian.

With regard to neutral particles that the Earth's atmosphere may be exposed to, the neutral interstellar He is the dominant constituent with its density outside the heliosphere of $\approx 1.5\ \mathrm{cm}^{-3}$ for cases 4 – 6 chosen here. In the focusing cone on the downwind side of the ISN flow the He density even exceeds 100 cm^{-3}. In terms of energy flux delivered to the upper atmosphere, the neutral solar wind is more important because of its much higher kinetic energy. On the upwind side both H and He contribute, with He containing more energy because of its higher mass. The total energy flux in the neutrals reaches almost 5% of that of the solar wind ions. On the downwind axis the dominant fraction of the energy flux is in the neutrals that are generated by charge exchange of He^+ pickup ions with interstellar He neutrals. It delivers approximately the full solar wind energy flux directly into the upper atmosphere.

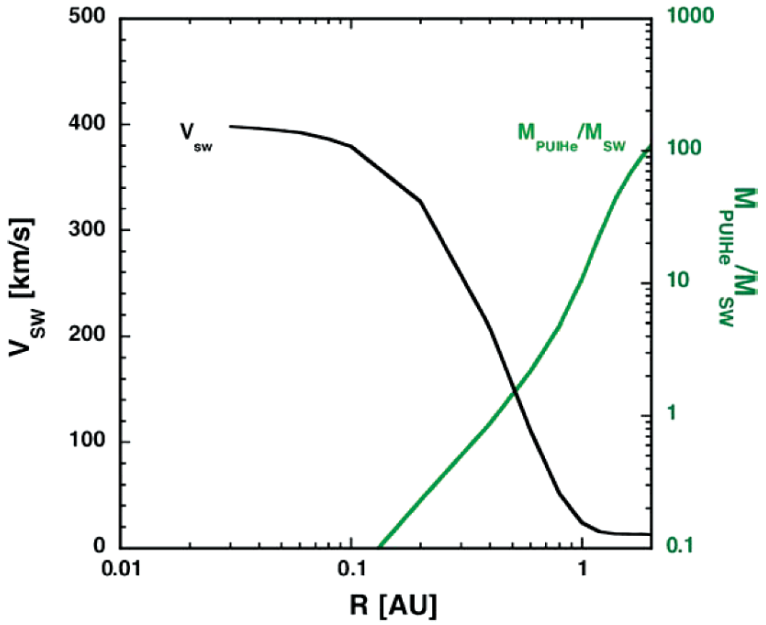

Figure 8.11. Radial evolution of the effective solar wind speed and the mass-loading by He^+ pickup ions on the downwind cone axis for case 5, assuming a homogeneous interaction between neutral He and the solar wind (Möbius et al., 2005).

On the upwind side the abundance of pickup He^+ reaches about 10% of the solar wind alpha particles and ≈ 1% of the solar wind protons at 1 AU, still not important for the solar wind dynamics. However, on the

cone axis pickup He^+ reaches the average solar wind density at 1 AU, with obvious impact on the solar wind dynamics. As discussed already above, the density of a tertiary product, pickup ions that turned neutral, becomes comparable with that of pickup ions here. These neutrals also carry away momentum from the solar wind, because they were originally accelerated on average to the solar wind speed and thus contributed to its mass-loading. Since both the interstellar neutral He and pickup ion densities are two orders of magnitude lower outside the cone, the neutrals generated from the pickup ions are negligible everywhere else. To demonstrate the order of magnitude of the solar wind slowdown due to the interaction with interstellar He in the density enhancement of the cone, Fig. 8.11 shows the radial evolution of the mass-loading ratio ($M_{PUI,He^+}/M_{SW}$) and the effective solar wind speed (v_{SW}), assuming a homogenous interstellar density. The mass-loading ratio has reached almost 10, and the solar wind has slowed down dramatically at 1 AU, as discussed by Möbius et al. (2005). At a distance of ≈3 AU from the Sun, the solar wind blends smoothly into the interstellar gas flow by approaching its speed of 13 km/s. To compute this estimate the loss of momentum to neutral solar wind and neutrals, which originate from He^+ pickup ions, was included, since they completely decouple dynamically from the solar wind flow. This momentum loss becomes important already at ≈ 0.3 AU. It should be noted though that the overall solar wind slowdown is overestimated, because the density enhancement in the cone is limited to a region that ranges from less than 1^o to approximately 5^o in both directions, depending on the interstellar gas flow speed. Through magnetic tension, the solar wind in the cone is still dynamically coupled to the region outside the cone, where the mass-loading is substantially weaker. As long as the solar wind speed outside the cone still exceeds the Alfvén velocity, the coupling to the surrounding medium is weak, because the information of the slowdown can only travel at the Alfvén velocity. Because this condition is mostly fulfilled at 1 AU outside the cone, the estimate given here for the solar wind slowdown in the cone is roughly representative of what can be expected under the conditions chosen here. For a more detailed evaluation, the cone needs to be treated like a comet in the solar wind (e.g. Schmidt and Wegmann, 1980; Schmidt et al., 1993). In a nutshell, the gravitational focusing cone in a dense cold interstellar gas cloud scenario will behave like a giant stationary cometary coma in the inner solar system (Möbius et al., 2005).

8.3.4 Energetic Particles of Interstellar Origin in the Inner Heliosphere

As has been discussed for the contemporary conditions in Section 8.2.5, pickup ions constitute a very important source population for energetic particles in the heliosphere. They are injected into further acceleration with an efficiency that exceeds by more than a factor of 100 that of solar wind ions. On average the abundance of interstellar He^+ is already 6% of the total energetic He population at 1 AU under current conditions (Kucharek et al., 2003). Even for the dense interstellar cloud conditions considered here (cases 4 – 6), He^+ pickup ions constitute only 1% of the total solar wind ion density, and they can still be treated mostly as test particles in the solar wind. Therefore, it is justified to estimate the expected energetic particle density that arises from acceleration of these pickup ions through linear scaling based on the increased pickup ion density. For an interstellar cloud with a He density of 1.5 cm^{-3} the average He^+/He^{2+} ratio in the energetic particles should grow to $n_{He+}/n_{He2+} \approx 6$, making He^+ dominant over He^{2+} in the energetic particle population.

Due to its enhancement in the focusing cone, the abundance of He will probably exceed that of H and become the dominant species of interplanetary accelerated particles on the downwind side of the ISM flow. Because pickup ions and, in particular, energetic particles are spatially much more widely distributed than their source, the energetic particle enhancement will spread well beyond the cone and become noticeable in Earth's orbit, even if the interstellar flow vector is not well aligned with the ecliptic plane.

During solar minimum, co-rotating interaction regions are the dominant generators of energetic particles and they accelerate interstellar pickup ions very efficiently (Gloeckler et al., 1996; Möbius et al., 2002). In CIRs $He^+/He^{2+} \approx 0.2$–0.25 on average at 1 AU, and about 20–25 times more He^+ than He^{2+} is expected under cold dense cloud conditions. Therefore, the flux of He^+ would exceed that of H^+ in CIRs even outside the focusing cone. If one includes the compounding effects of the focusing cone, pickup ions will play the dominant role as a source of energetic particles during solar minimum conditions. Assuming that the solar wind and solar activity conditions remain similar to what is observed in

the contemporary heliosphere, the abundance of interstellar pickup ions will boost the total flux of energetic particles in general, at least under solar minimum conditions. Since also the intensity of ACRs is substantially increased throughout the entire heliosphere (Fahr et al., this volume) and modulation of galactic cosmic rays will be significantly reduced because of the smaller heliosphere dimensions (Florinski and Zank, this volume), the total energetic particle fluxes around the Earth will be substantially enhanced over the entire energy range. Therefore, the change in the energetic particle spectra and fluxes around Earth is probably one of the most important effects of a moderately enhanced ISM density on the Earth's environment.

Acknowledgments: The authors would like to thank the International Space Science Institute (ISSI) for hosting a coordination meeting for the work towards the manuscript. E. M. would like to thank the staff at ISSI and at the Physics Institute of the University of Bern during part of the preparation of this chapter and thankfully acknowledges support by the Hans-Sigrist Stiftung. The authors thank M.A. Lee and the reviewer for carefully reading the manuscript and helpful suggestions. The work by E. M. was supported under NASA grants NAG5-12929 and NAG5-10890, H.-R. M. was supported under NASA grants NAG5-12879 and NAG5-13611, and M. B. under the Polish SCSR grant 1P03D00927.

REFERENCES

Adams, T.F., and Frisch, P.C. (1977). High-resolution observations of the Lyman-α sky background. *Astrophys. J.*, 212:300–308.

Ajello, J.M., Pryor, W.R., Barth, C.A., Hord, C.W., Stewart, A.I.F., Simmons, K.E., and Hall, D.T. (1994). Observations of interplanetary Lyman-alpha with the Galileo Ultraviolet Spectrometer: Multiple scattering effects at solar maximum. *Astron. Astrophys.*, 289:283–303.

Akasofu, S.-I., (1964a). A source of the energy for geomagnetic storms and auroras. *Planet. Space Sci.*, 12:801–833.

Akasofu, S.-I, (1964b). The neutral hydrogen flux in the solar plasma flow. *Planet. Space Sci*., 12: 905–913.

Axford, W.I., (1972). The interaction of the solar wind with the interstellar medium, In Sonnett, E.P., Coleman, P. J., Wilcox, J. M. Editors, *Solar Wind*, NASA SP-308, pages 609–660.

Bamert, K., Wimmer-Schweingruber, R.F., Kallenbach, R., Hilchenbach, M., Klecker, B., Bogdanov, A., and Wurz, P., (2002). Origin of the May 1998 suprathermal particles: Solar and heliospheric observatory/Charge, Element, and Isotope Analysis Sys-

tem/(Highly) Suprathermal Time of Flight results, *J. Geophys. Res.,* 107:1130, 10.1029/2001JA900173.

Banks, P.M., (1971). Interplanetary hydrogen and helium from cosmic dust and the solar wind. *J. Geophys. Res.,* 76:4341–4348.

Baranov, V.B., and Malama, Yu.G., (1993). Model of the solar wind interaction with the Local Interstellar Medium: numerical solution of self-consistent problem. *J. Geophys. Res.,* 98:15157–15163.

Barnett, C.F., Hunter, H.T., Kirkpatrick, M.I., Alvarez, I., Cisneros, C., and Phaneuf, R.A., (1990). Collisions of H, H_2, He and Li atoms and ions with atoms and molecules, In: *Atomic data for fusion*. Oak Ridge National Laboratories, ORNL-6086/V, Oak Ridge, Tenn.

Bertaux, J.-L., and Blamont, J.E., (1971). Evidence for a source of an extraterrestrial hydrogen Lyman-alpha emission: the interstellar wind. *Astron. Astrophys.,* 11:200–217.

Bertaux, J. L., Lallement, R., Kurt, V. G., and Mironova, E. N., (1985). Characteristics of the local interstellar hydrogen determined from PROGNOZ 5 and 6 interplanetary Lyman-alpha line profile measurements with a hydrogen absorption cell. *Astron. Astrophys*., 150:1–20.

Breus, T.K., Bauer, S.J., Krymskii, A.M., and Mitnitskii, V.Ya., (1989). Mass loading in the solar wind interaction with Venus and Mars. *J. Geophys*., Res., 94:2375–2382.

Burlaga, L.F., Ness, N.F., Belcher, J.W., and Whang, Y.C., (1996). Pickup protons and pressure-balanced structures from 39 to 43 AU: Voyager 2 observations during 1993 and 1994, *J. Geophys. Res*., 101:15523–15254.

Bzowski, M., Fahr, H.J., and Rucinski, D. (1996). Interplanetary neutral particle fluxes influencing the Earth's atmosphere and the terrestrial environment, *Icarus* 124:209–219.

Bzowski, M., (2001). Time-dependent radiation pressure and time dependent, 3D ionisation rate for heliospheric modelling, In Scherer, K., Fichtner, H., Fahr, H.J., Marsch E., Editors, *The Outer Heliosphere: The Next Frontier*, COSPAR Coll. Ser., 11:69–72, Elsevier, Pergamon.

Chassefière, E., Bertaux, J.-L., Lallement, R., and Kurt, V.G. (1986). Atomic hydrogen and helium densities of the interstellar medium measured in the vicinity of the sun. *Astron. Astrophys.*, 160:229–242.

Chotoo, K., Schwadron, N.A., Mason, G.M., Zurbuchen, T.H., Gloeckler, G., Posner, A., Fisk, L.A., Galvin, A.B.; Hamilton, D.C. and Collier, M.R., (2000). The suprathermal seed population for corotating interaction region ions at 1 AU deduced from composition and spectra of H^+, He^{++}, and He^+ observed on Wind. *J. Geophys. Res.,* 105:23107–32122.

Clarke, J.T., Lallement, R., Bertaux, J.L., Fahr, H.-J., Quémerais, E., and Scherer, H. (1998). HST/GHRS observations of the velocity structure of interplanetary hydrogen. *Astrophys. J.,* 499:482–488.

Collier, M.R., Moore, T.E., Ogilvie, K.W., Chornay, J.D., Keller, J.W., Boardsen, S., Burch, J.L., El Marji, B., Fok, M.-C., Fuselier, S.A., Ghielmetti, A.G., Giles, B.L., Hamilton, D.C., Peko, B.L., Quinn, J.M., Stephen, T.M., Wilson, G.R., and Wurz, P., (2001). Observations of neutral Atoms from the Solar Wind. *J. Geophys. Res.,* 106:24893–24906.

Collier, M.R., Moore T.E., Ogilvie, K., Chornay, D.J., Keller, J., Fuselier, S., Quinn, J., Wurz, P., Wuest, M., and Hsieh, K.C., (2003). Dust in the wind: The dust geometric cross section at 1 AU based on neutral solar wind observations, Solar Wind X. *American Institute Physics.,* 679:790–793.

Collier, M.R., Moore, T.E., Simpson, D., Roberts, A., Szabo, A., Fuselier, S., Wurz, P., Lee, M.A., and Tsurutani, B., (2004). An unexplained 10º– 40º shift in the location of some diverse neutral atom data at 1 AU. *Adv. Space Res.,* 34:166–171.

Costa, J., Lallement, R., Quémerais, E., Bertaux, J.-L., Kyrölä, E., and Schmidt, W., (1999). Heliospheric interstellar H temperature from SOHO/SWAN H cell data. *Astron. Astrophys.,* 349:660–672.

Fahr, H.-J., (1968a) On the Influence of Neutral Interstellar Matter on the Upper Atmosphere, *Astrophys. Space Sci*., 2:474–495.

Fahr, H.J., (1968b). Neutral corpuscular energy flux by charge-transfer collisions in the vicinity of the sun. *Astrophys. Space Sci*., 2:496–503.

Fahr, H.J., (1974). The extraterrestrial UV-background and the nearby interstellar medium. *Space Sci. Rev.,* 15:483–540.

Fahr, H.J., Lay, G. and Wulf-Mathies, C. (1978). Derivation of interstellar helium gas parameters

Fahr, H.J., (1979). Interstellar hydrogen subject to a net repulsive solar force field *Astron. Astrophys.,* 77:101–109.

Fahr, H.J., Ripken, H.W., and Lay, G., (1981). Plasma-Dust Interactions in the Solar Vicinity and their Observational Consequences. *Astron. Astrophys*., 102:359–370.

Fahr, H.J. (1991). Local interstellar oxygen in the heliosphere: its analytic representation and observational consequences, *Astron. Astrophys.*, 241:251–259.

Fahr, H.J., and Rucinski, D. (1999). Neutral interstellar gas atoms reducing the solar wind Mach number and fractionally neutralizing the solar wind, *Astron. Astrophys*. 350:1071–1078.

Fahr, H.J., and Rucinski, D. (2001). Modification of properties and dynamics of distant solar wind due to its interaction with neutral interstellar gas, *Space Sci. Rev*., 97:407–412.

Fahr, H.-J. (2004). Global structure of the heliosphere and interaction with the local interstellar medium: three decades of growing knowledge, Adv. Space Sci., 34:3–13.

Fahr, H.-J., Fichtner, H., Scherer, K., and Stawicki, O. (2005). Variable terrestrial particle environments during the galactic orbit of the sun, In: P. C. Frisch Editor, *Solar Journey: The Significance of Our Galactic Environment for the Heliosphere and Earth.* This Volume, Springer, Dordrecht.

Florinski, V., and Zank, G. P. (2005). Variations in the galactic cosmic ray intensity in the heliosphere in response to variable interstellar environments, In: P. C. Frisch Editor, *Solar Journey: The Significance of Our Galactic Environment for the Heliosphere and Earth*. This Volume, Springer, Dordrecht.

Flynn, B., Vallerga, J., Dalaudier, F., and Gladstone, G.R. (1998). EUVE measurements of the local interstellar wind and geocorona via resonance scattering of solar He I 584-Å line emission, *J. Geophys. Res*., 103:6483–6494.

Frisch, P.C., Dorschner, J.M., Greenberg, J.M., Grün, E., Landgraf, M., Hoppe, P., Jones, A.P., Krätschmer, W., Linde, T.J., Morfill, G.E., Reach, W., Slavin, J.D., Svestka, J., Witt, A.N., Zank, G.P., (1999). Dust in the Local Interstellar Wind, *Astrophys. J.*, 525:492–516.

Frisch, P.C., and Slavin, J. (2003). The Chemical Composition and Gas-to-Dust Mass Ratio of Nearby Interstellar Matter. *Astrophys. J.,* 594:844–858.

Frisch, P.C., (2000). The galactic environment of the Sun. *J. Geophys. Res.,* 105:10279–10290.

Frisch, P.C., and Slavin, J. (2005) Short-term variations in the galactic environment of the Sun, In: P. C. Frisch Editor, *Solar Journey: The Significance of Our Galactic Environment for the Heliosphere and Earth*. This Volume, Springer, Dordrecht.

Gangopadhyay, P., Izmodenov, V., Gruntman, M., and Judge, D.L. (2002). Interpretation of Pioneer 10 Ly-β based on heliospheric interface models: Methodology and first results, *J. Geophys. Res.,* 107:doi:10.1029/2002JA009345.

Gangopadhyay, P., Izmodenov, V.V., Quemerais, E., Gruntman, M.A., and Judge, D.L., Interpretation of Pioneer 10 and Voyager 2 Ly alpha data: first results, *Adv. Space Res.,* 34:94–98.

Geiss, J., Gloeckler, G., and von Steiger, R., (1996). Origin of C^+ Ions in the Heliosphere. *Space Sci. Rev.,* 78:43–52.

Gloeckler, G., Geiss, J., Balsiger, H., Fisk, L.A., Galvin, A.B., Ipavich, F.M., Ogilvie, K.W., von Steiger, R., and Wilken, B., (1993). Detection of interstellar pick-up hydrogen in the Solar System. *Science,* 261:70–73.

Gloeckler, G., Geiss, J., Roelof, E.C., Fisk, L.A., Ipavich, F.M., Ogilvie, K.W., Lanzerotti, L.J., von Steiger, R., and Wilken, B., (1994). Acceleration of interstellar pickup ions in the disturbed solar wind observed on Ulysses. *J. Geophys. Res.,* 99:17637–17643.

Gloeckler, G., Jokipii, J.R., Giacalone, J., and Geiss, J., (1994). Concentration of interstellar pickup H^+ and He^+ in the solar wind. *Geophys. Res. Lett.,* 21:1565–1568.

Gloeckler, G., Schwadron, N.A., Fisk, L.A., and Geiss, J., (1995). Weak pitch angle scattering of few MV rigidity ions from measurements of anisotropies in the distribution function of interstellar pickup H^+. *Geophys. Res. Lett.,* 22:19:2665–2668.

Gloeckler, G., (1996). The abundance of atomic ^{1}H, ^{4}He and ^{3}He in the local interstellar cloud from pickup ions observations with SWICS on Ulysses. *Space Sci. Rev.,* 78:335–346.

Gloeckler, G., and Geiss, J., (1998). Interstellar and inner source pickup ions observed with SWICS on Ulysses. *Space Sci. Rev.,* 86:127–159.

Gloeckler, G., (1999). Observation of injection and pre-acceleration processes in the slow solar wind. *Space Sci. Rev.,* 89:91–104.

Gloeckler, G., Fisk, L.A., Geiss, J., Schwadron, N.A., and Zurbuchen, T.H., (2000). Elemental composition of the inner source pickup ions. *J. Geophys. Res.,* 105:7459–7463.

Gloeckler, G., and Geiss, J., (2001). Heliospheric and interstellar phenomena deduced from pickup ions. *Space Sci. Rev.,* 97:169–181.

Gloeckler, G., Möbius, E., Geiss, J., Bzowski, M., Rucinski, D., Terasawa, T., Noda, H., Oka, M., McMullin, D.R., Skoug, R., Chalov, S., Fahr, H., von Steiger, R., Yamazaki, A., and Zurbuchen, T., (2004). Observations of the Helium Focusing Cone with Pickup Ions. *Astron. Astrophys.,* 426:845–854.

Grün, E., Gustafsson, B.A.S., Mann, I., Baguhl, M., Morfill, G., Staubach, P., Taylor, A., and Zoog, H.A. (1994). Interstellar dust in the heliosphere. *Astron. Astrophys.*, 286:915–924.

Gruntman, M.A. (1994). Neutral solar wind properties: Advance warning of major geomagnetic storms. *J. Geophys. Res*., 99:19213–19227.

Gruntman, M.A. (1997). Energetic neutral atom imaging of space plasmas. *Rev. Sci. Instr.,* 68:3617–3656.

Gruntmann, M.A., Roelof, E.C., Mitchell, D.G., Fahr, H.J., Funsten, H.O., and McComas, D.J. (2001). Energetic neutral atom imaging of the heliospheric boundary region. J. Geophys. Res., 106:15767–15782.

Hilchenbach, M., Grünwaldt, H., Kallenbach, R., Klecker, B., Kucharek, H., Ipavich, F.M. and Galvin, A.B., (1999). Observation of suprathermal helium at 1 AU: Charge states in CIRs, in: *Solar Wind Nine*. ed. Habbal et al., 605–608.

Holzer, T.E., (1977). Neutral hydrogen in interplanetary space. *Rev. Geophys. and Space Phys.,* 15:467–490.

Holzer, T.E., and Axford, I. (1971). Interaction between interstellar helium and the solar wind, *J. Geophys. Res.*, 76:6965-6970.

Hovestadt, D., Gloeckler, G., Klecker, B., and Scholer, M., (1984a). Ionic charge state measurements during He^{+}-rich solar energetic particle events. *Astrophys. J.,* 281:463–467.

Hovestadt, D., Klecker, B., Scholer, M., Gloeckler, G., and Ipavich, F.M., (1984b), Survey of He^{+}/He^{2+} abundance ratios in energetic particle events, *Astrophys. J.*, 282:L39–L42.

Illing, R.M.E., and Hildner, E., (1994) Neutral hydrogen in the solar wind at 1 AU, *Eos Trans. AGU,* 75(16):261.

Izmodenov, V.V., Geiss, J., Lallement, R., Gloeckler, G., Baranov, V.B., and Malama, Yu.G. (1999). Filtration of interstellar hydrogen in the two-shock heliospheric interface: Inferences on the LIC electron density. *J. Geophys. Res*., 104:4731–4741.

Izmodenov, V.V., Gruntman, M.A., and Malama, Yu.G., (2001). Interstellar hydrogen atom distribution function in the outer heliosphere. *J. Geophys. Res.,* 106:10681–10689.

Izmodenov, V., Malama, Y.G., Gloeckler, G. and Geiss, J. (2004). Filtration of interstellar H, O, N atoms through the heliospheric interface: Inferences on local interstellar abundances of the elements, *Astron. Astrophys*., 414:L29–L32.

Kucharek, H., Möbius, E., Li, W., Farrugia, C.J., Popecki, M.A., Galvin, A.B., Klecker, B., Hilchenbach, M., and Bochsler, P. (2003). On the source and the acceleration of energetic He^{+}: Long term observations with ACE/SEPICA. *J. Geophys. Res.,* 108:8030, doi:10.1029/2003.JA009938.

Lallement, R., (1996). Relations between ISM inside and outside the heliosphere. *Space Sci. Rev.*, 78:361–374.

Lallement, R., Raymond, C.J., Vallerga, J., Lemoine, M., Dalaudier, F., and Bertaux, J.L., (2004a). Modeling the interstellar-interplanetary helium 58.4 nm resonance glow: Towards a reconciliation with particle measurements. *Astron. Astrophys.,* 426:875–884.

Lallement, R., Raymond, J.C., Bertaux, J.-L., Quémerais, E., Ko, Y.-K., Uzzo, M., McMullin, D., and Rucinski, D., (2004b). Solar cycle dependence of the helium focusing cone from SOHO/UVCS observations. *Astron. Astrophys.,* 426:867–874.

Lallement, R. Quémerais, E. Bertaux, J.L. Ferron, S. Koutroumpa, D. and Pellinen, R. (2005). Deflection of the Interstellar Neutral Hydrogen Flow Across the Heliospheric Interface, *Science*, 307:1449–1451.

Landgraf, M. (2000). Modeling the motion and distribution of interstellar dust inside the heliosphere. *J. Geophys. Res.*, 105:10303–10316.

Landgraf, M., Krüger, H., Altobelli, N., and Grün, E. (2003). Penetration of the heliosphere by the interstellar dust stream during solar maximum. *J. Geophys. Res.*, 108:8030 doi:10.1029/2003JA009872.

Landgraf, M. (2005). Variations in interstellar dust distribution in the heliosphere, In: P. C. Frisch Editor, *Solar Journey: The Significance of Our Galactic Environment for the Heliosphere and Earth*. This Volume, Springer, Dordrecht.

Lee, M.A. (1997). Effects of cosmic rays and interstellar gas on the dynamics of a wind, in: *Cosmic Winds and the Heliosphere*, eds. J.R. Jokipii, C.P. Sonett, and M.S. Giampapa, pp. 857–886.

Levasseur-Regourd, A.C., Renard, J.B., and Dumont, R., (1991). The zodiacal cloud complex, In: A.C. Levasseur-Regourd and Hasegawa, H. Editors, *Origin and Evolution of Interplanetary Dust*. Pages 131–138, Kluwer Academic Publishers.

Maher, L.J., and Tinsley, B.A., (1977). Atomic hydrogen escape due to charge exchange with hot plasmaspheric ions. *J. Geophys. Res.,* 82:689–695.

Mann, I., Kimura, H., Biesecker, D.A., Tsurutani, B.T., Grün, E., McKibben, B., Liou, J.-C., MacQueen, R.M., Mukai, T., Guhathakurta, L., and Lamy, P., (2004). Dust near the Sun. *Space Sci. Rev.,* 110:269–305.

Marsch, E., Pilipp, W.G., Thieme, K.M., and Rosenbauer, H. (1989). Cooling of solar wind electrons inside 0.3 AU. *J. Geophys. Res.,* 94:6893–6898.

McComas, D., Allegrini, F., Bochsler, P., Bzowski, M., Collier, M., Fahr, H., Fichtner, H., Frisch, P., Funsten, H., Fuselier, S., Gloeckler, G., Gruntman, M., Izmodenov, V., Knappenberger, P., Lee, M., Livi, S., Mitchell, D., Moebius, E., Moore, T., Reisenfeld, D., Roelof, E., Schwadron, N., Wieser, M., Witte, M., Wurz, P., and Zank, G., (2004). The Interstellar Boundary Explorer (IBEX). *AIP Conference Proceedings*. 719:162–181.

McMullin, D., McMullin, D.R., Bzowski, M., Möbius, E., Pauluhn, A., Skoug, R., W.T., Thompson, Witte, M., von Steiger, R., Rucinski, D., Banaszkiewicz, M., and Lallement, R., (2004). Heliospheric conditions that affect the interstellar gas inside the heliosphere. *Astron. Astrophys.,* 426:885–895.

Möbius, E., Hovestadt, D., Klecker, B., Scholer, M., G.,Gloeckler and Ipavich, F.M., (1985). Direct observation of He^+ pick-up ions of interstellar origin in the solar wind. *Nature*. 318:426–429.

Möbius, E., Klecker, B., Hovestadt, D., and Scholer, M., (1988). Interaction of interstellar pick-up ions with the solar wind. *Astrophys. Space Sci.*, 144:487–505.

Möbius, E. (1993). Gases of Non-Solar Origin in the Solar System. In: *Landoldt-Börnstein, Numerical Data and Functional Relationships in Science and Technology*, VI/3A Chapter 3.3.5.1, pp. 184–188.

Möbius, E., Rucinski, D., Hovestadt, D., and Klecker, B., (1995). The helium parameters of the very local interstellar medium as derived from the distribution of He^+ pickup ions in the solar wind. *Astron. Astrophys.,* 304:505–519.

Möbius, E., Rucinski, D., Lee, M.A., and Isenberg, P.A., (1998). Decreases in the antisunward flux of interstellar pickup He^+ associated with radial interplanetary magnetic field. *J. Geophys. Res.* 103:257–265.

Möbius, E., Morris, D., Popecki, M.A., Klecker, B., Kistler, L.M., and Galvin, A.B., (2002). Charge States of Energetic Ions Obtained from a Series of CIRs in 1999 – 2000 and Implications on Source Populations. *Geophys. Res. Lett.,* 29, 10.1029/2001GL013410.

Möbius, E., Bzowski, M., Chalov, S., Fahr, H.-J., Gloeckler, G., Izmodenov, V., Kallenbach, R., Lallement, R., McMullin, D., Noda, H., Oka, M., Pauluhn, A., Raymond, J., Rucinski, D., Skoug, R., Terasawa, T., Thompson, W., Vallerga, J., von Steiger, R., and Witte, M., (2004). Synopsis of the interstellar He parameters from combined neutral gas, pickup ion and UV scattering observations and related consequences. *Astron. Astrophys*., 426:897–907.

Möbius, E., Bzowski, M., Müller, H.-R., and Wurz, P., (2005). Impact of Dense Interstellar Gas Clouds on the Neutral Gas and Secondary Particle Environment in the Inner Heliosphere, in: Proceedings of the Solar Wind 11/SOHO 16 Conference, T. Zurbuchen and B. Fleck eds., *ESA Special Publication*, SP-592, 367–370.

Morris, D., Möbius, E., Lee, M,A., Popecki, M.A., Klecker, B., Kistler, L.M., and Galvin, A.B., (2001). Implications for Source Populations of Energetic Ions in Co-Rotating Interaction Regions from Ionic Charge States, in: Solar and Galactic Composition, *AIP Conference Proceedings*, 598:201–204.

Müller, H.-R., Zank, G. P., and Lipatov, A. S. (2000). Self-consistent hybrid simulations of the interaction of the heliosphere with the local interstellar medium. *J. Geophys. Res*., 105:27419–27438.

Oka, M., Terasawa, T., Noda, H., Saito, H., and Mukai, T., (2002). Torus Distribution of Interstellar Pickup Ions: Direct Observation. *Geophys. Res. Lett*., 29:1612–1615.

Osterbart, R., and Fahr, H.-J. (1992). A Boltzmann-kinetic approach to describe the entrance of neutral interstellar hydrogen into the heliosphere, *Astron.Astroph ys.,* 264:260–269.

Paresce, F., Bowyer, S., and Kumar, S. (1974). Observations of He I 584 □ nighttime radiation; evidence for an interstellar source of neutral helium. *Astrophys. J.*, 187:633–639.

Parker, E.N. (1963) Interplanetary Dynamical Processes, *Interscience Monographs and Texts in Physics and Astronomy*, Wiley & Sons, New-York, Vol. VIII, pp. 126–127.

Parker, E.N. (2005) Interstellar conditions and planetary magnetospheres, In: P.C. Frisch Editor, *Solar Journey: The Significance of Our Galactic Environment for the Heliosphere and Earth*. This Volume, Springer, Dordrecht.

Pilipp, W.G., Miggenrieder, H., Montgomery, M.D., Mühlhäuser, K.-H., Rosenbauer, H., and Schwenn, R. (1987a). Characteristics of electron velocity distribution functions in the solar wind derived from the Helios plasma experiment. *J. Geophys. Res.,* 92:1075–1092.

Pilipp, W.G., Miggenrieder, H., Montgomery, M.D., Mühlhäuser, K.-H., Rosenbauer, H., and Schwenn, R. (1987b). Variations of electron distribution functions in the solar wind. *J. Geophys. Res.,* 92:1103–1118.

Quemerais, E., Bertaux, J.-L., Sandel, B. R., and Lallement, R., (1994). A new measurement of the interplanetary hydrogen density with ALAE/ATLAS 1. *Astron. Astrophys*. 290:941–955.

Quemerais, E.; Bertaux, J.L., Lallement, R., Berthé, M., Kyrölä, E., and Schmidt, W. (1999). Interplanetary Lyman a line profiles derived from SWAN/SOHO hydrogen cell measurements: Full-sky vector field. *J. Geophys. Res.*, 104:12585–12603.

Ragot, B.R., and Kahler, S.W. (2003). Interactions of dust grains coronal mass ejections and solar cycle variations of the F-corona brightness. *Astrophys. J.*, 594:1049 –1059.

Richardson, J.D., Paularena, K.I., Lazarus, A.J., and Belcher, J.W. (1995). Evidence for a solar wind slowdown in the outer heliosphere? *Geophys. Res. Lett*., 22:1469–1472.

Ripken, H.W., and Fahr, H.-J. (1983). Modification of the local gas properties in the heliospheric interface. *Astron. Astrophys.*, 122:181–192.

Rosenbauer, H., Fahr, H.J., Keppler, E., Witte, M., Hemmerich, P., Lauche, H., Loidl, A., and Zwick, R., (1983). ISPM Interstellar Neutral Gas Experiment. *ESA SP-1050*, pp. 125–139.

Richter, I., Leinert, C., and Planck, B., (1982). Search for the variations of Zodiacal Light and optical detection of interplanetary plasma clouds. *Astron. Astrophys.*, 110:115–120.

Rucinski, D., Cummings, A.C., Gloeckler, G., Lazarus, A.J., Möbius, E., and Witte, M., (1996). Ionization processes in the heliosphere – Rates and methods of their determination. *Space Sci. Rev.,* 78:73–84.

Rucinski, D., and Fahr, H.J., (1989). The influence of electron impact ionization on the distribution of interstellar helium in the inner heliosphere; possible consequences for determination of interstellar helium parameters. *Astron. Astrophys*., 224:290–298.

Rucinski, D., and Fahr, H.J., (1991). Nonthermal ions of interstellar origin at different solar wind conditions. *Ann.Geophys.*, 9:102–110.

Rucinski, D., Bzowski, M., and Fahr, H.J., (2003). Imprints from the solar cycle on the helium atom and helium pick-up ion distributions. *Ann.Geophys*., 21:1315 –1330.

Saul, L., Möbius, E., Smith, C.W., Bochsler, P., Grünwaldt, H., Klecker, B., and Ipavich, F.M., (2004). Observational Evidence of Pitch Angle Isotropization by IMF Waves. *Geophys. Res. Lett*., 31:L05811 10.1029/2003GL019014.

Schmidt, H. U., and Wegmann, R., (1980). MHD–Calculations for Cometary Plasmas. *Comp. Phys. Comm*., 19:309–326.

Schmidt, H. U.; Wegmann, R., and Neubauer, Fritz M., (1993). MHD modeling applied to Giotto encounter with comet P/Grigg-Skjellerup. *J. Geophys. Res*., 98:21, 009–21,016.

Schwadron, N.A., Zurbuchen, T.H., Fisk, L.A., and Gloeckler, G., (1999). Pronounced enhancements of pickup hydrogen and helium in high-latitude compressional regions. *J. Geophys. Res.,* 104:535–548.

Spitzer, L. (1978). *Physical Processes in the Interstellar Medium*. John Wiley & Sons, New York.

Strömgren, E. (1939). The physical state of interstellar hydrogen, *Astrophys. J.*, 89:526–547.

Szegö, K., Glassmeier, K.-H., Brinca, A., Cravens, T., Fischer, C., Fisk, L., Gombosi, T., Haerendel, G., Lee, M.A., Mazelle, C., Möbius, E., Motschmann, U., Isenberg, P., Sauer, K., Schwadron, N., Shapiro, V., Tsurutani, B., and Zank,, G., (2000). Physics of Mass Loaded Plasmas. *Space Sci. Rev.,* 94:429 –671.

Thomas. G.E., and Krassa, R.F., (1971). OGO 5 measurements of the Lyman Alpha sky background. *Astron. Astrophys*. 11:218–233.

Vallerga, J., Lallement, R., Lemoine, M., Dalaudier, F., and McMullin, D., (2004). EUVE observations of the helium glow: Interstellar and solar parameters. *Astron. Astrophys.,* 426:855–865.

Vasyliunas,V.M., and Siscoe, G.L., (1976). On the flux and the energy spectrum of interstellar ions in the solar system. *J. Geophys. Res*. 81:1247–1252.

Wang, C., and Richardson, J.D., (2003). Determination of the solar wind slowdown near solar maximum. *J. Geophys. Res.* 108:1058 10.1029/2002JA009322.

Weinberg, J.L., (1964). The zodiacal light at 5300 Å, *Ann. Astrophys*. 27: 718–738.

Weller, C.S., and Meier, R.R. (1974). Observations of helium in the interplanetary /interstellar wind: the solar-wake effect. *Astrophys. J.,* 193:471–476.

Welty, D.E., Hobbs, L.M., Lauroesch, J. T., Morton, D. C., Spitzer, L., and York, D. G. (1999). The Diffuse Interstellar Clouds toward 23 Orionis. *Astrophys. J. Suppl.*, 124:465–501.

Wieser, M., Wurz, P., Bochsler, P., Moebius, E., Quinn, J., Fuselier, S.A., Ghielmetti, A., DeFazio, J., Stephen, T.M., and Nemanich, R.J. (2005). NICE: An Instrument for Direct Mass spectrometric Measurement of Interstellar Neutral Gas. *Meas. Sci. Technol*. 16: 1667–1676.

Wimmer-Schweingruber, R. F., and Bochsler, P. (2001). Lunar Soils - An Archive for the Galactic Environment of the Solar System? In Wimmer-Schweingruber, R., Editor, *Solar and Galactic Composition*, *AIP Conference Proceedings*, 598:399–402.

Wimmer-Schweingruber, R. F., and Bochsler, P., (2003). On the origin of inner-source pickup ions. *Geophys. Res. Lett*., 30:1077–1080.

Witte, M., (2004). Kinetic parameters of interstellar neutral helium. *Astron. Astrophys.,* 426:835–844.

Witte, M., Banaszkiewicz, M., Rosenbauer, H., and McMullin, D., (2004). Kinetic parameters of interstellar neutral helium: updated results from the ULYSSES/GAS-instrument. *Adv. Space Res.,* 34:61–65.

Wood, B.E., Linsky, J. L., and Zank, G.P. (2000). Heliospheric, astrospheric, and interstellar Ly-α absorption toward 36 Ophiuchi, *Astrophys. J.*, 537:304–311.

Wu, F.M., and Judge, D.L. (1979). Temperature and velocity of the interplanetary gases along solar radii. *Astrophys. J.*, 231:594–605.

Wurz, P., Collier, M.R., Moore, T.E., Simpson, D., Fuselier, S., and Lennartson, W. (2004). Possible Origin of the Secondary Stream of Neutral Fluxes at 1 AU. *AIP Conference Proceedings* 719:195–200.

Yeghikyan, A., and Fahr, H.-J. (2004). Terrestrial atmospheric effects induced by counterstreaming dense interstellar cloud material. *Astron. Astrophys.,* 425:1113–1118.

Yeghikyan, A., and Fahr, H.-J. (2005) Accretion of interstellar material into the heliosphere and onto Earth, In: P. C. Frisch Editor, *Solar Journey: The Significance of Our Galactic Environment for the Heliosphere and Earth*. This Volume, Springer, Dordrecht.

Zank, G.P., and Frisch, P.C. (1999). Consequences of a Change in the Galactic Environment of the Sun. *Astrophys. J.*, 518:965–997.

Zank, G.P., et al. (2005). Variations in the heliosphere in response to variable interstellar material, In: P. C. Frisch Editor, *Solar Journey: The Significance of Our Galactic Environment for the Heliosphere and Earth*. This Volume, Springer, Dordrecht.